Viscoelasticity and generalized Stokes–Einstein relations of colloidal dispersions

Adolfo J. Banchio and Gerhard Nägele[a)]
Fakultät für Physik, Universität Konstanz, Postfach 5560, D-78457 Konstanz, Germany

Johan Bergenholtz
Department of Physical Chemistry, Göteborg University, S–412 96 Göteborg, Sweden

The linear viscoelastic and diffusional properties of colloidal model dispersions are investigated and possible relations between the (dynamic) shear viscosity and various diffusion coefficients are analyzed. Results are presented for hard sphere and charge-stabilized dispersions with long-range screened Coulomb interactions. Calculations of the dynamic long-time properties are based on a (rescaled) mode coupling theory (MCT). For hard sphere suspensions a simple hydrodynamic rescaling of the MCT results is proposed which leads to good agreement between the theory and experimental data and Brownian dynamics simulation results. The rescaled MCT predicts that the zero-shear limiting viscosity of hard sphere dispersions obeys nearly quantitative generalized Stokes–Einstein (GSE) relations both with regard to the long-time self-diffusion coefficient and the long-time collective diffusion coefficient measured at the principal peak of the static structure factor. In contrast, the MCT predicts that the same GSEs are violated in the case of dispersions of highly charged particles. The corresponding short-time GSEs are found to be partially violated both for charged and uncharged colloidal spheres. A frequency dependent GSE, relating the elastic storage and viscous loss moduli to the particle mean squared displacement, is also investigated, According to MCT, this GSE holds fairly well for concentrated hard spheres, but not for charge-stabilized systems. Remarkably good agreement is obtained, however, with regard to the frequency dependence of the Laplace-transformed reduced shear stress relaxation function and the Laplace-transformed reduced time-dependent self-diffusion coefficient for both charged and uncharged particle dispersions. © *1999 American Institute of Physics.* [S0021-9606(99)50541-2]

I. INTRODUCTION

The prediction of rheological and diffusional transport coefficients of colloidal suspensions from microscopic models is a major theoretical challenge. It is important to develop an understanding of the microscopic origins of these properties to aid, e.g., in the modeling of more complex and industrially relevant dispersions. The calculation of colloidal transport properties from first principles is complicated because of the presence of long-range many-body hydrodynamic interactions (HI) mediated by the intervening solvent. The presence of HI distinguishes colloidal systems from simple liquids in which the molecular motion is ballistic and is determined only by the intermolecular force law.

Of particular technological relevance is the viscoelastic behavior of colloidal dispersions, characterized by the real part, $\eta'(\omega)$, and imaginary part, $\eta''(\omega)$, of the complex-valued dynamic viscosity $\eta(\omega)$. The function $\eta(\omega)$ determines the macroscopic stress induced in a suspension upon the application of a low-amplitude oscillatory shear strain of frequency ω (cf. Sec. II). The dynamic viscosity and its zero-frequency limit, the zero-shear limiting suspension viscosity, η, have been determined experimentally for a variety of colloidal systems using mechanical rheometers.[1–8]

In contrast, diffusional properties like the short-time and long-time collective and self-diffusion coefficients, particle mean square displacements (MSDs), and the dynamic structure factor, $S(q,t)$, are nearly always determined using dynamic light scattering (DLS) techniques.[9,10] For an infinitely dilute suspension, the shear viscosity η becomes equal to the solvent viscosity η_0 that is related to the single particle diffusion coefficient D_0 by the well-known Stokes–Einstein relation $D_0 = k_B T/(6\pi\eta_0 a)$, where a is the radius of a spherical colloidal particle.

In concentrated dispersions and in dilute dispersions with long-range particle interactions, particle diffusion is slowed down due to potential and hydrodynamic particle interactions. Furthermore, the suspension viscosity can be substantially larger than the infinite dilution value η_0. As a consequence of these interactions, the Stokes-Einstein formula no longer represents the particle diffusivity. In monodisperse suspensions of correlated particles, one needs now to distinguish between self-diffusion and collective diffusion coefficients, depending on whether the Brownian motion of a tagged particle or the density relaxation involving the simultaneous motion of many particles is considered. Moreover, the viscosity and the diffusion coefficients associated with the short-time regime $t \ll \tau_a$ have to be distinguished from the corresponding quantities for the long-time regime $t \gg \tau_a$. Here, $\tau_a = a^2/D_0$ is the time required for a noninter-

[a)]Corresponding author, electronic mail: gerhard.naegele@uni-konstanz.de

acting spherical particle of radius a to diffuse a distance comparable to its own size.

Many attempts have been made in the past to connect experimentally the rheological and diffusional transport processes of concentrated colloidal suspensions.[1–3,7,11,12] The idea underlying these attempts is that both processes reflect relaxation by diffusion in response to a structural deformation caused by an applied flow or by the diffusing particles themselves. These types of studies have led to a number of empirical generalized Stokes–Einstein (GSE) relations in which a diffusional property correlates with a rheological property.[1,2,12,13]

One well-known example, studied extensively in the past as a function of the particle volume fraction, Φ, is the GSE between the zero-shear limiting shear viscosity η and the long-time self-diffusion coefficient D_S^L, given by

$$\frac{\eta(\Phi)}{\eta_0} = \frac{D_0}{D_S^L(\Phi)}. \tag{1}$$

The Φ dependence of these quantities is made explicit in Eq. (1). This GSE has been explored for hard sphere dispersions,[14–18] surfactant systems,[19] and protein dispersions.[20] Although this GSE works reasonably well in a qualitative sense for these systems, experiments by Imhof and co-workers[12] revealed that it is a poor approximation for charge-stabilized dispersions. However, for concentrated hard sphere dispersions near the (idealized mode coupling) glass transition concentration, Fuchs et al. have verified the GSE in Eq. (1) using the MCT predictions for the α-relaxation scaling regime.[21,22] According to their calculations, $(D_S^L/D_0)(\eta/\eta_0) \approx 0.94$.[22]

It is worth noting that there is no obvious theoretical reason to expect Eq. (1) to hold in an extended concentration regime since η can be is expressed as a time integral over a transverse stress autocorrelation function [cf. Eq. (38)], whereas D_S^L can be expressed in terms of the Green-Kubo formula,

$$D_S^L = \frac{1}{3} \int_0^\infty dt \langle \mathbf{V}(t) \cdot \mathbf{V}(0) \rangle, \tag{2}$$

over the velocity autocorrelation function of a representative particle with velocity $\mathbf{V}$, which is obviously a one-particle property.

Segrè and co-workers[2] used a two-color DLS technique and viscometric measurements of η to identify another GSE which appears to be nearly quantitative for hard sphere dispersions for particle volume fractions up to the freezing transition. Their experimental results show that the shear viscosity of a hard sphere dispersion scales quantitatively according to

$$\frac{\eta(\Phi)}{\eta_0} = \frac{D_0}{D_C^L(q_m;\Phi)}, \tag{3}$$

with the reciprocal of the so-called long-time collective diffusion coefficient, $D_C^L(q_m)$, measured at a wave number, q_m, corresponding to the peak position of the maximum of the static structure factor, $S(q)$. The coefficient $D_C^L(q_m)$ is

determined experimentally by noting that for long correlation times $t \gg \tau_a$, $S(q_m,t)$ decays exponentially as[2]

$$S(q_m,t) \approx S(q_m)e^{-q_m^2 D_C^L(q_m)t}. \tag{4}$$

While long-time structural relaxation over distances $2\pi/q_m$ and inverse viscosity might be expected to show similar dependences on concentration, there is again no obvious reason to expect the GSE in Eq. (3) to hold quantitatively. Through its dependence on the long-time form of $S(q_m,t)$, the diffusion coefficient $D_C^L(q_m)$ is linked to a time integral over the longitudinal (i.e., not transversal as it is the case for η) stress autocorrelation function, evaluated now at a finite wave number q_m. In fact, while the GSE has been established experimentally for colloidal hard spheres (and appears to hold also for other types of colloidal–like systems[23]), recent mode coupling theory (MCT) calculations[13] suggest that the same GSE does not hold for salt-free charge-stabilized suspensions of spherical particles (cf. also Sec. V). It follows that these calculations predict that Eq. (3) does not provide a universal quantitative relation for concentrated dispersion independent of the type of particle interaction.

Further GSEs arise from considering the short-time versions of Eqs. (1) and (3), i.e.,[7]

$$\frac{\eta_\infty'(\Phi)}{\eta_0} = \frac{D_0}{D_S^S(\Phi)}, \tag{5}$$

and

$$\frac{\eta_\infty'(\Phi)}{\eta_0} = \frac{D_0}{D_C^S(q_m;\Phi)}. \tag{6}$$

In these short-time GSEs, $\eta_\infty' = \eta(\omega \to \infty)$ is the high frequency limiting shear viscosity (cf. Sec. II), and D_S^S is the short-time self-diffusion coefficient. Furthermore, $D_C^S(q_m)$ is the short-time collective diffusion coefficient associated with the short-time relaxation of the dynamic structure factor at wave number q_m. The short-time form of $S(q_m,t)$ is given by Eq. (4), with $D_C^L(q_m)$ replaced by $D_C^S(q_m)$ and $t \ll \tau_a$. The diffusion coefficient D_S^S is a purely hydrodynamic property quantifying the small-displacement mobility of a tracer particle in the equilibrium dispersion. Correspondingly, the high frequency viscosity η_∞' reflects viscous dissipation due to a high frequency, low-amplitude shear oscillation in the linear viscoelastic regime. The short-time properties of η_∞', D_S^S, and $D_C^S(q_m)$ are related to the diffusive motion on time scales that are long relative to the momentum relaxation and fluid vorticity diffusion times, but short relative to the structural relaxation time τ_a.

Experimental work of Shikata and Pearson[3] and of Zhu and co-workers[11] on hard sphere suspensions support the short-time GSE in Eq. (5) within experimental accuracy, whereas theoretical calculations (cf. Sec. V B) and computer simulations[24,25] suggest that there are measurable differences between η_∞'/η_0 and D_0/D_S^S. For charge-stabilized systems with intermediate high salt content, Bergenholtz and co-workers[7] showed experimentally that η_∞'/η_0 lies above $(D_S^S/D_0)^{-1}$ for all volume fractions considered. In Sec. V B we examine theoretically the short-time GSE in Eq. (5) for both hard sphere and salt-free charge-stabilized dispersions,

as well as the short-time version in Eq. (6) of the long-time GSE of Segrè *et al.*[2] for neutral and charged colloidal spheres.

So far no test has been provided for the short-time version in Eq. (6) of the long-time GSE of Segrè *et al.*[2] Such a test will be provided in Sec. V B, for both neutral and charged colloidal spheres.

An interesting heuristic extension of the GSEs in Eqs. (1) and (5) to finite strain frequencies has been proposed by Mason and Weitz.[1] According to them, an approximate GSE,

$$\frac{\tilde{\eta}(s)}{\eta_0} \approx \frac{D_0}{s^2 \tilde{W}(s)} = \frac{D_0}{s \tilde{D}(s)}, \tag{7}$$

exists between the dynamic viscosity, $\tilde{\eta}(s)$, in the Laplace domain, with

$$\tilde{\eta}(s) = \eta(s = i\omega) = \eta'_\infty + \int_0^\infty dt\, \Delta\eta(t) e^{-st}, \tag{8}$$

and the Laplace transform,

$$\tilde{D}(s) = \int_0^\infty dt\, e^{-st} D(t) = s\tilde{W}(s) \tag{9}$$

of the self-diffusion function $D(t) = dW(t)/dt$. Here, $W(t) = \langle [\mathbf{R}(t) - \mathbf{R}(0)]^2 \rangle/6$ is the MSD of a representative particle with position vector $\mathbf{R}$. Equation (7) is supposed to hold for frequencies s in the Laplace domain sufficiently small so that inertial effects are not resolved. In Eq. (8) $\Delta\eta(t)$ is the shear stress relaxation function associated with noninstantaneous stress relaxations (cf. Sec. II).

Since $\tilde{\eta}(s \to 0) = \eta$ and $\tilde{\eta}(s \to \infty) = \eta'_\infty$, as well as $\lim_{s \to 0} s\tilde{D}(s) = D_S^L$ and $\lim_{s \to \infty} s\tilde{D}(s) = D_S^S$, Eq. (7) reduces to the GSEs in Eqs. (1) and (5) in the zero-frequency and high-frequency limits, respectively. Mason and Weitz have tested Eq. (7) experimentally for a variety of systems, including polymer networks and a concentrated metastable hard sphere dispersion.[1,26] For these systems they find good qualitative, albeit not quantitative agreement with Eq. (7). Besides Eq. (7) we will discuss in Sec. V C another frequency dependent GSE related to the Mason and Weitz GSE.

From a practical point of view, the GSE in Eq. (7) is quite intriguing: if it were to hold for a variety of particle pair potentials, then $\eta'(\omega)$ and $\eta''(\omega)$ could be determined over a very large frequency regime using dynamic light scattering techniques. In contrast, the accessible frequency range of conventional rheometers is far more restricted. It is therefore of relevance to investigate the general validity of the Mason and Weitz GSE. Such an investigation is performed in Sec. V C over an extended range of volume fractions for both colloidal hard spheres and charge-stabilized suspensions located in the fluid regime.

The purpose of this article is twofold: first we provide a thorough discussion of the differences and similarities of the viscoelastic and diffusional behavior of hard sphere dispersions and of charge-stabilized dispersions of spherical particles with long-range potential interactions. Several long-time and short-time rheological properties (within the limit of small applied strain) and diffusional quantities are calcu-

lated and discussed. Comparisons with experiments and computer simulations are made to assess the accuracy of our theoretical predictions.

Second, we employ a (rescaled) mode coupling theory for the calculation of long-time rheological and diffusional properties, and we explore in detail its predictions with regard to the GSEs introduced here in Sec. I. In this work, we make use of an idealized version of the mode coupling theory. This type of MCT was developed several years ago for the description of the dynamics of simple liquids.[21,27–29] It was later recognized that this theory is particularly well suited to study the glass transition because the slowing down of the dynamics and structural arrest is captured through certain bifurcation scenarios that appear in the self-consistent long-time solution of the MCT equations.[21,30–33] Furthermore, the results of the MCT have been shown to be in accord with experimental measurements of the dynamics of concentrated colloidal hard spheres near the glass transition.[33–38]

Recently, starting from the Smoluchowski equation describing colloidal dynamics, we have attempted to include the effect of hydrodynamic interactions within the framework of the original MCT, in anticipation of their importance in colloidal systems with particle concentrations below the glass transition. This inclusion of HI has been accomplished for the far-field, pairwise additive part of the HI, for both monodisperse suspensions[39] and multicomponent colloidal mixtures;[40–42] it can be used to determine the properties of suspensions for which near-field HI are not important, such as de-ionized suspensions of charged particles. For hard sphere suspensions where many-body HI is important even at moderate densities, we employ a semi-empirical hydrodynamic short-time rescaling procedure in the spirit of Medina-Noyola[43] and of Brady[16,17] to approximate the effect of HI on the particle dynamics. The outcome of our theoretical treatment is compared with results from experiments and Brownian dynamics (BD) computer simulations. For an alternative treatment of the effect of HI within the MCT framework see Ref. 44. The results presented in this work will demonstrate that the (rescaled) MCT is a versatile tool for determining a large number of dynamic properties of concentrated colloidal dispersions.

This article is organized as follows: in Sec. II pertinent relations and concepts associated with the general theory of linear viscoelasticity of colloidal dispersions are introduced. Section II also includes a discussion of the asymptotic behavior of various viscoelastic properties. For charge-stabilized suspensions, the well-known concept of the effective hard sphere fluid model is introduced, as is commonly done in the analysis of soft sphere suspensions,[8–10] which allows a simplified qualitative and physically intuitive description of, in particular, short-time dynamic quantities. In Sec. III, we summarize and discuss the self-consistent coupled MCT equations used for numerically calculating the structural part of the linear viscoelastic functions and diffusional properties of neutral and charged particle dispersions. The limiting behavior of the viscoelastic functions obtained from MCT is established in Sec. IV and compared with known exact results. We examine in Sec. IV the nonlinear

volume fraction dependence of short-time diffusional properties of salt-free charge-stabilized suspensions, and compare it with corresponding results for hard sphere dispersions. These short-time quantities are used in Sec. V A for the exploration of the short-time GSEs.

Numerical results for the viscoelastic and diffusional properties of hard sphere and salt-free charge-stabilized dispersions are presented and discussed in Sec. V. Comparisons are made with experimental data and computer simulation results. Section V A contains the (rescaled) MCT results for the viscoelastic functions and the shear viscosity. The validity of the frequency independent GSEs introduced here is investigated in Sec. V B on the basis of our numerical and analytical results. The accuracy of the frequency dependent Mason and Weitz GSE is analyzed in Sec. V C using the (rescaled) MCT. Our final conclusions are contained in Sec. VI.

II. LINEAR VISCOELASTICITY: GENERAL RELATIONS

Here in Sec. I we summarize some pertinent relations in the theory of linear viscoelasticity of colloidal dispersions. These relations will be needed in the ensuing analysis.

We consider a homogeneous suspension of spherical particles subjected to a weak oscillatory fluid flow of frequency ω and shear rate amplitude $\dot{\gamma}$. More explicitly, the ambient oscillatory fluid velocity field is assumed to be given by the real part of

$$\mathbf{u}(\mathbf{r},t) = \dot{\gamma} y \hat{\mathbf{x}} e^{i\omega t} \tag{10}$$

with the Peclet number $\text{Pe} = \dot{\gamma}\tau_a \ll 1$. Here, $\hat{\mathbf{x}}$ is the unit vector in x-direction and ω is the frequency of the applied strain. The Newtonian shear viscosity of the solvent is denoted by η_0. For $\text{Pe} \ll 1$, the suspension is only slightly distorted from its isotropic equilibrium microstructure, and there exists thus a linear relation between the xy component, $\Sigma_{xy}(t)$, of the macroscopic suspension stress tensor at time t and the shear rate amplitude $\dot{\gamma}$. This relation is[40]

$$\Sigma_{xy}(t) = \dot{\gamma}\left[\eta'_\infty e^{i\omega t} + \int_{-\infty}^{t} d\tau \Delta\eta(t-\tau) e^{i\omega\tau} \right]$$
$$= \Sigma_{xy}^H(t) + \Sigma_{xy}^T(t), \tag{11}$$

where η'_∞ is the high frequency limiting viscosity and $\Delta\eta(t)$ is the shear stress relaxation function describing the noninstantaneous stress relaxation of the slightly shear-distorted microstructure. Both quantities η'_∞ and $\Delta\eta(t)$ are taken within the limit of vanishing shear rate. According to Eq. (11), there are two distinct contributions to the shear stress $\Sigma_{xy}(t)$. On the time scale of interest, the hydrodynamic part $\Sigma_{xy}^H(t)$ of the shear stress follows the applied strain rate $\dot{\gamma}\cos(\omega t)$ instantaneously, giving rise to the high frequency limiting shear viscosity η'_∞.[8,45] This is a purely hydrodynamic quantity that is due to the particles being nondeformable. To first order in the volume fraction $\Phi = (4/3)na^3$, where n is the number density of particles, η'_∞ is given by the well-known Einstein result $\eta'_\infty/\eta_0 = 1 + 2.5\Phi$. The noninstantaneous so-called thermodynamic contribution $\Sigma_{xy}^T(t)$ to the macroscopic shear stress lags behind the strain rate and arises from Brownian and potential equilibrium restoring

forces.[8,45] These forces resist the flow-induced distortion and strive to retain the isotropic equilibrium microstructure. The noninstantaneous relaxation of the shear-distorted microstructure towards equilibrium is described by the shear relaxation function $\Delta\eta(t)$.

Equation (11) can be rewritten in terms of the complex-valued dynamic shear viscosity $\eta(\omega)$ as

$$\Sigma_{xy}(t) = \eta(\omega)\dot{\gamma}e^{i\omega t}, \tag{12}$$

where

$$\eta(\omega) = \int_0^\infty dt\, e^{-i\omega t}\eta(t) = \eta'(\omega) - i\eta''(\omega) \tag{13}$$

is the Fourier-Laplace transform of the total shear stress relaxation function $\eta(t) = 2\eta'_\infty\delta(t) + \Delta\eta(t)$ which accounts also for the instantaneous hydrodynamic part proportional to the delta function $\delta(t)$. The dynamic shear viscosity $\eta(\omega)$ is related to the complex-valued dynamic shear modulus $G(\omega)$ via

$$G(\omega) = G'(\omega) - iG''(\omega) = i\omega\eta(\omega), \tag{14}$$

where

$$G'(\omega) = \omega\eta''(\omega) = \omega\int_0^\infty dt\,\sin(\omega t)\Delta\eta(t) \tag{15}$$

is the frequency dependent elastic storage modulus and

$$G''(\omega) = \omega\eta'(\omega) = \omega\left[\eta'_\infty + \int_0^\infty dt\,\cos(\omega t)\Delta\eta(t) \right] \tag{16}$$

denotes the viscous loss modulus. The real part $\eta'(\omega)$ is in phase with the oscillatory rate of strain and accounts for the dissipated energy, whereas the phase-shifted part $\eta''(\omega)$ measures the elastically stored energy. Notice that $\eta''(\omega)$ is in phase with the applied strain $\dot{\gamma}\sin(\omega t)$. Purely viscous behavior corresponds to $\eta'' = 0$, whereas purely elastic behavior, aside from the high frequency contribution η'_∞, corresponds to $\eta' - \eta'_\infty = 0$. For intermediate to high-frequency strain there is enough time for the system to restore isotropic equilibrium during one cycle and elastic energy is stored in the distorted configuration: the system behaves like a viscoelastic fluid. Within the limit of large frequencies, there is no structural relaxation at all and consequently no accompanying dissipation of energy. Therefore, the high frequency limit of the complex shear viscosity is determined completely by hydrodynamic interactions. Indeed, from Eq. (11) it follows at large frequencies that

$$\Sigma_{xy}(t) \approx \dot{\gamma}\left[\eta'_\infty - i\frac{G'_\infty}{\omega} \right]e^{i\omega t}, \tag{17}$$

provided that $\omega\tau_a \gg 1$ and provided that the high frequency limiting elastic shear modulus $G'_\infty = G'(\omega\to\infty)$ exists. The limit $\omega\to\infty$ should be understood as $\tau_a^{-1} \ll \omega \ll \tau_\eta^{-1}$ where $\tau_\eta = \rho a^2/\eta_0$ is the time required for an overdamped viscous shear wave to diffuse a distance equal to the particle radius. In the above, ρ is the mass density of the solvent. As a consequence, the high frequency regime corresponds to the short-time regime described by the Smoluchowski equation.[9,40,45] The upper bound on ω guarantees that inertial

effects are absent in the particle dynamics and that solvent-mediated hydrodynamic interactions can be considered to act instantaneously between the particles. The high-frequency modulus G'_∞ exists provided that the shear relaxation function $\Delta\eta(t)$ is regular at $t=0$, i.e., in the short-time regime $\tau_\eta \ll t \ll \tau_a$. For a regular $\Delta\eta(t)$, G'_∞ is given by

$$G'_\infty = \Delta\eta(t=0). \tag{18}$$

There are instances where G'_∞ does not exist. For a suspension of hard spheres without HI, it has been shown[46,47] that $G'(\omega)$ grows asymptotically without bounds as $\omega^{1/2}$, corresponding to $\Delta\eta(t)$, diverging like $t^{-1/2}$ for $t\to0$. As was derived in Ref. 47, the exact short-time form of the reduced shear relaxation function of a hard sphere dispersion in the absence of HI is given by

$$\frac{\tau_a \Delta\eta(t)}{\eta_0} \approx \frac{18}{5}\Phi^2 \sqrt{\frac{2}{\pi}} g(2a^+)\left(\frac{t}{\tau_a}\right)^{-1/2}, \tag{19}$$

provided that $t \ll \tau_a$. Here, $g(2a^+)$ is the contact value of the hard sphere radial distribution function for which accurate analytic expressions are known. The singular short-time behavior of $\Delta\eta(t)$ implies an asymptotic high frequency behavior of the shear moduli according to

$$\frac{\tau_a}{\eta_0}G'(\omega) \approx \frac{18}{5}\Phi^2 g(2a^+)(\omega\tau_a)^{1/2}, \tag{20}$$

and

$$\frac{\tau_a}{\eta_0}G''(\omega) \approx \frac{18}{5}\Phi^2 g(2a^+)(\omega\tau_a)^{1/2} + \frac{\eta'_\infty}{\eta_0}\omega\tau_a, \tag{21}$$

with $\omega\tau_a \gg 1$. A finite plateau value G'_∞ of $G'(\omega)$ is recovered, however, when near-field HI is accounted for.[18,47] Near-field HI causes the relative mobility of two spherical particles to vanish upon contact.[48]

The high frequency limiting modulus G'_∞ remains finite also for suspensions with soft long-range repulsive interactions, where the effect of the physical hard core is completely masked, such as in charge-stabilized suspensions with low salinity.

At zero frequency, Eq. (11) reduces to

$$\Sigma_{xy} = \dot{\gamma}\eta, \tag{22}$$

where η is the zero-frequency suspension viscosity. In this work, we focus on the contribution,

$$\eta - \eta'_\infty = \Delta\eta = \int_0^\infty dt\,\Delta\eta(t), \tag{23}$$

to the shear viscosity due to noninstantaneous stress relaxations. As far as η'_∞ is concerned, Lionberger and Russel[47] provide a semi-empirical expression for hard sphere suspensions which covers the entire concentration range. This expression is

$$\frac{\eta'_\infty}{\eta_0} = \frac{1+1.5\Phi(1+\Phi-0.189\Phi^2)}{1-\Phi(1+\Phi-0.189\Phi^2)}, \tag{24}$$

and it agrees well with measured values of η'_∞ for hard sphere dispersions and conforms to the exact low density

result up to quadratic order [cf. Eq. (25)]. Furthermore, η'_∞ diverges at the value $\Phi=0.64$ where random close packing occurs.

Exact numerical values for the low shear limiting viscosity η of hard sphere suspensions are known only up to quadratic order in Φ, i.e., $\eta = \eta'_\infty + \Delta\eta$ with[49,50]

$$\frac{\eta'_\infty}{\eta_0} = 1 + \frac{5}{2}\Phi + 5\Phi^2 + \mathcal{O}(\Phi^3), \tag{25}$$

and

$$\frac{\Delta\eta}{\eta_0} = 0.913\Phi^2 + \mathcal{O}(\Phi^3). \tag{26}$$

When the HI are neglected, $\Delta\eta$ is given instead by[8,46]

$$\frac{\Delta\eta}{\eta_0} = \frac{12}{5}\Phi^2 + \mathcal{O}(\Phi^3). \tag{27}$$

For dilute suspensions of strongly repelling charge-stabilized particles, HI can be treated as a pairwise additive and η'_∞ is well approximated by[8,51]

$$\frac{\eta'_\infty}{\eta_0} = 1 + \frac{5}{2}\Phi + \frac{5}{2}\Phi^2 + \frac{15}{2}\Phi^2 \int_0^\infty dx\, x^2 g(x) J(x), \tag{28}$$

with $J(x) \approx \frac{15}{2}x^{-6}$ for $x=r/a \gg 1$. The integral on the right-hand side of Eq. (28) is a number of at most the order of 1. Hence η'_∞/η_0 is expected to be well approximated by the Einstein result for $\Phi \ll 1$.

Previous work[10,52–54] has revealed that the dilute limiting behavior of short-time transport properties of low-salt charge-stabilized suspensions is modified due to the long-range repulsion among the particles. This leads to a qualitatively different volume fraction dependence compared to hard spheres. However, the Einstein term in the virial-type expansion of the high frequency viscosity is a single particle property; it is unaffected by particle correlations, which are the source of often fractional Φ dependence of, e.g., the (short-time) sedimentation velocity and the short-time self-diffusion coefficient [cf. Eq. (70)]. As a consequence, the Einstein term $\eta'_\infty/\eta_0 = 1 + 2.5\Phi$ is always, i.e., regardless of the pair potential, a good approximation provided the volume fraction is sufficiently small.

This point is clarified further by crudely approximating the radial distribution function $g(x)$ of a charge-stabilized system by the zero-density form $g_{EHS}^{(0)}(x)=\Theta(x-2b/a)$ of an effective hard sphere (EHS) system. The effective radius $b>a$ is assumed to be substantially larger than the hydrodynamic radius a. Here, $\Theta(x)$ is the unit step function. The effective volume fraction Φ_{eff} is related to the physical one by $\Phi_{eff}=\Phi(b/a)^3$. The effective particle radius b accounts for the electrostatic repulsion between the particles and can be identified as $b=r_m/2$, where r_m is the principal peak position of the actual $g(r)$. For the present case of salt-free suspensions of strongly charged particles, r_m coincides to within 3% of the average geometrical distance $\bar{r}=a(4\pi/3\Phi)^{1/3}$ of two particles.[55] Using the effective zero density $g(x)$ in Eq. (28) with $b=\bar{r}/2$, we obtain

$$\frac{\eta'_\infty}{\eta_0} = 1 + \frac{5}{2}\Phi + \frac{5}{2}\Phi^2 + 4.48\Phi^3. \tag{29}$$

The zero-density form of $g(x)$ for the effective hard sphere model used in deriving Eq. (29) can be improved to $g_{EHS}(x) = 2(b/a)A(\Phi_{eff})\delta(x-2b/a) + \Theta(x-2b/a)$ by adding a delta-function term which accounts for the well-developed first maximum of the $g(r)$ of charged particles. The dimensionless function $A(\Phi_{eff})$ is determined from the compressibility equation[56]

$$1 + n\int d^3r[g(r)-1] = \frac{\chi_T(\Phi_{eff})}{\chi_T^{id}}, \tag{30}$$

where $\chi_T(\Phi_{eff})$ is the isothermal compressibility calculated using the Carnahan-Starling equation of state,[56] and $\chi_T^{id} = (nk_BT)^{-1}$ is the corresponding ideal gas value. Again using $b = \bar{r}/2$ and hence $\Phi_{eff} = \pi/6$, it follows that $A(\Phi_{eff}) = 0.25$. As a result, the prefactor 4.48 in the cubic term in Eq. (29) increases to 7.90 when the delta term contribution is considered. Since the prefactor of the cubic term is of the order of one, Eq. (29) reduces indeed to Einstein's low density result for $\Phi \ll 1$. It should be stressed that, contrary to hard sphere dispersions, the $g(r)$ of charge-stabilized colloids can exhibit strong oscillations even for volume fractions as low as 10^{-4}.[10]

It will be convenient for later discussion to introduce the reduced dynamic viscosities[4,50]

$$R(\omega) = \frac{\eta'(\omega) - \eta'_\infty}{\eta - \eta'_\infty}, \tag{31}$$

and

$$I(\omega) = \frac{\eta''(\omega)}{\eta - \eta'_\infty}, \tag{32}$$

that correspond to the real and imaginary parts of $\eta(\omega)$. The quantities $R(\omega)$ and $I(\omega)$ vary between 0 and 1. As we will show in Sec. V, $R(\omega)$ equals unity at $\omega = 0$, and it decays monotonically to zero with increasing frequency. The function $I(\omega)$ vanishes for $\omega \to 0$ and $\omega \to \infty$, exhibiting a broad maximum at intermediate frequencies.

III. CALCULATION OF VISCOELASTIC AND DIFFUSIONAL PROPERTIES

We proceed now to establish an exact expression for the shear relaxation function with HI included, together with a Green-Kubo formula for the static shear viscosity. The exact expression for $\Delta\eta(t)$ is the basis for a self-consistent mode coupling theory for the linear viscoelastic functions and for the dynamic structure factor $S(q,t)$. The latter is defined as[9]

$$S(q,t) = \left\langle \frac{1}{N}\sum_{l,p=1}^N e^{i\mathbf{q}\cdot(\mathbf{R}_l(t)-\mathbf{R}_p(0))} \right\rangle, \tag{33}$$

where $\mathbf{q}$ is the wave vector with modulus q, and $\mathbf{R}_l(t)$ is the center-of-mass position vector of particle l at time t. The equilibrium average of the unsheared suspension is denoted by $\langle\cdots\rangle$. The function $S(q,t)$ includes information on the diffusional properties and is the key property determined in DLS experiments.[9,10] The many-body HI effects on the par-

ticle dynamics in concentrated hard sphere dispersions will be accounted for using a semi-empirical hydrodynamic scaling procedure. Since a full account of the derivation of the exact Green-Kubo formula for η and for the MCT equations determining $S(q,t)$ and $\Delta\eta(t)$ has been given in Refs. 40–42, we will discuss only the final results and some of their implications. The predictions of the (rescaled) MCT will be explored Secs. IV and V.

Using a projection operator formalism and linear response theory based on the many-particle Smoluchowski equation, two of the present authors have derived an exact expression for the shear relaxation function within the limit of small shear rates.[40] As derived in Ref. 40, $\Delta\eta(t)$ can be expressed as an equilibrium stress autocorrelation function,

$$\Delta\eta(t) = \frac{1}{k_BTV}\langle\hat{\sigma}^{xy}e^{t\hat{\Omega}^\dagger}\hat{\sigma}^{xy}\rangle, \tag{34}$$

with the xy component of the microscopic stress tensor given by

$$\hat{\sigma}^{xy} = \sum_{i=1}^N \left([R_i^x\delta_{y\gamma} + C_i^{xy\gamma}(\mathbf{R}^N)]\frac{\partial U(\mathbf{R}^N)}{\partial R_i^\gamma} \right.$$
$$\left. - k_BT\frac{\partial}{\partial R_i^\gamma}C_i^{xy\gamma}(\mathbf{R}^N) \right). \tag{35}$$

In the above equation, R_i^γ is the γth Cartesian component of $\mathbf{R}_i$ out of N particles in the system volume V, and summation over repeated Cartesian indexes is implied. Moreover,

$$\hat{\Omega}^\dagger(\mathbf{R}^N) = \sum_{i,j=1}^N \left(\nabla_i - \frac{1}{k_BT}\nabla_iU(\mathbf{R}^N) \right)\cdot\mathbf{D}_{ij}(\mathbf{R}^N)\cdot\nabla_j \tag{36}$$

is the adjoint Smoluchowski operator of an unsheared suspension, and $U(\mathbf{R}^N)$ is the total potential energy of the colloidal particles. The hydrodynamic diffusivity tensor $\mathbf{D}_{ij}(\mathbf{R}^N)$ depends in general on the particle position configuration $\mathbf{R}^N = (\mathbf{R}_1,\ldots,\mathbf{R}_N)$, and it relates the hydrodynamic force on particle i to the resulting drift velocity on particle j. The function $C_i^{\alpha\beta\gamma}(\mathbf{R}^N)$ is a Cartesian component of the third rank shear mobility tensor $\mathbf{C}_i(\mathbf{R}^N)$ which accounts for the shear-induced hydrodynamic interaction of particle i with the remaining particles. For a force- and torque-free sphere i advected by the ambient flow field as described in Eq. (10), the αth component of the convective velocity $\mathbf{V}_i(\mathbf{R}^N,t)$ is given by[40,45]

$$V_i^\alpha(\mathbf{R}^N,t) = \dot{\gamma}[R_i^y\delta_{x\alpha} + C_i^{xy\alpha}(\mathbf{R}^N)]\cos(\omega t). \tag{37}$$

We emphasise that $\langle(\cdots)\rangle = \int d\mathbf{R}^N P_{eq}(\mathbf{R}^N)(\cdots)$ is the equilibrium average with respect to the equilibrium distribution function $P_{eq}(\mathbf{R}^N)$ in the absence of shear flow. Explicit analytical expressions for the hydrodynamic tensors $\mathbf{D}_{ij}(\mathbf{R}^N)$ and $\mathbf{C}_i(\mathbf{R}^N)$ are available only on the two-body level in terms of inverse distance expansions.[57,58]

From Eq. (34) we conclude that η can be written in terms of a Green-Kubo formula,

$$\eta - \eta'_\infty = \frac{1}{k_BTV}\int_0^\infty dt\langle\hat{\sigma}^{xy}e^{t\hat{\Omega}^\dagger}\hat{\sigma}^{xy}\rangle. \tag{38}$$

J. Chem. Phys., Vol. 111, No. 18, 8 November 1999

Viscoelasticity of colloidal dispersions   8727

The high-frequency modulus is then identified using Eq. (18) as

$$G'_\infty = \frac{1}{k_B TV} \langle (\hat{\sigma}^{xy})^2 \rangle. \tag{39}$$

These expressions have proven useful for calculating the low-shear rate viscosity[59] and high-frequency shear modulus[60] using Stokesian dynamics computer simulations.

Without HI, $\mathbf{D}_{ij} = D_0 \delta_{ij} \mathbf{1}$, where $\mathbf{1}$ is the three-dimensional unit tensor, and $\mathbf{C}_i = 0$. As discussed in Ref. 40, the Green–Kubo formula in Eq. (38) agrees then formally, aside from an irrelevant kinetic contribution, with a corresponding expression for the shear viscosity of a simple atomic liquid. However, it should be recalled that the time evolution in colloidal dispersions is governed by the irreversible Smoluchowski equation instead of by the Liouville equation. Consequently, $\Delta \eta(t)$, like any regular autocorrelation function obeying Smoluchowski dynamics, decays monotonically towards zero as long as the system is located in the fluid regime of the phase diagram. The expression in Eq. (39) for G'_∞ is particularly useful since it allows a direct numerical calculation of G'_∞ with many-body HI included using a Monte Carlo generation of particle configurations (see Ref. 24 for such a determination of η'_∞).

Since $\Delta \eta(t)$ is given in terms of an equilibrium average in Eq. (34), it provides an ideal and rigorous starting point from which to formulate a mode coupling theory of linear viscoelasticity. A detailed derivation of the coupled equations for $\Delta \eta(t)$ and $S(q,t)$ with the inclusion of the pairwise additive far-field part of the HI and the extension to colloidal mixtures was presented in Refs. 40–42. In the absence of HI, the MCT equation determining $\Delta \eta(t)$ is

$$\Delta \eta(t) = \frac{k_B T}{60 \pi^2} \int_0^\infty dq q^4 \left[\frac{1}{S(q)} \frac{d}{dq} S(q) \right]^2 \left[\frac{S(q,t)}{S(q)} \right]^2, \tag{40}$$

where $S(q) = S(q, t=0)$ is the static structure factor related to the pair correlation function $g(r)$. Equation (40) for $\Delta \eta(t)$ is formally identical to the corresponding MCT expression for a one-component simple fluid.[61] For simple fluids there is, of course, no additional viscous contribution $2\eta'_\infty \delta(t)$ to the total shear relaxation function $\eta(t)$.

We note that Verberg, de Schepper and co-workers[62,63] have evaluated Eq. (40) by substituting a simple exponential form for $S(q,t)$, consistent with the short- and expected long-time limiting behavior, but at the expense of sacrificing the inherent self-consistency of the MCT. This, in turn, precludes the possibility of obtaining a glass transition and a corresponding divergence of the shear viscosity. Notice that $\Delta \eta(t)$ is uniquely determined through $S(q,t)$ and $S(q)$.

Without HI, $S(q,t)$ follows self-consistently from solving the coupled set of equations (see, e.g., Refs. 13, 42, 44, and 64),

$$\frac{\partial}{\partial t} S(q,t) = -q^2 D_C^S(q) S(q,t)$$

$$- \int_0^t du M_C^{\text{irr}}(q, t-u) \frac{\partial}{\partial u} S(q,u), \tag{41}$$

with the irreducible collective memory function,

$$M_C^{\text{irr}}(q,t) = \frac{nD_0}{2(2\pi)^3} \int d^3k [V^c(\mathbf{q},\mathbf{k})]^2 S(k,t) S(|\mathbf{q}-\mathbf{k}|,t), \tag{42}$$

and the vertex amplitude,[21,31,39,65]

$$V^C(\mathbf{q},\mathbf{k}) = \hat{\mathbf{q}} \cdot \mathbf{k} c(k) + \hat{\mathbf{q}} \cdot (\mathbf{q}-\mathbf{k}) c(|\mathbf{q}-\mathbf{k}|), \tag{43}$$

related to collective diffusion. Here, $c(q) = [1 - 1/S(q)]/n$ is the Fourier-transformed two-body direct correlation function, and $D_C^S(q)$ is the q-dependent short-time collective diffusion coefficient. Without HI the following result holds: $D_C^S(q) = D_0/S(q)$.

There exists an additional set of MCT equations determining the self-intermediate scattering function

$$G(q,t) = \langle e^{i\mathbf{q} \cdot (\mathbf{R}_1(t) - \mathbf{R}_1(0))} \rangle, \tag{44}$$

which contains information on self-diffusion. This set is explicitly[39,41,64]

$$\frac{\partial}{\partial t} G(q,t) = -q^2 D_S^S G(q,t)$$

$$- \int_0^t du M_S^{\text{irr}}(q, t-u) \frac{\partial}{\partial u} G(q,u), \tag{45}$$

with the irreducible memory function,

$$M_S^{\text{irr}}(q,t) = \frac{D_0}{(2\pi)^3 n} \int d^3k (\hat{\mathbf{q}} \cdot \mathbf{k})^2 [V^S(k)]^2 S(k,t)$$

$$\times G(|\mathbf{q}-\mathbf{k}|,t), \tag{46}$$

related to self-diffusion and the vertex amplitude given without HI by

$$V^S(k) = 1 - \frac{1}{S(k)}. \tag{47}$$

In Eq. (45), D_S^S is the short-time self-diffusion coefficient equal to the initial slope of the particle mean squared displacement $W(t)$. For vanishing HI, D_S^S reduces to D_0. The MSD is determined by[39,41]

$$W(t) = D_S^S \left[t - \int_0^t du (t-u) \Delta V(u) \right], \tag{48}$$

where $\Delta V(t)$ is essentially the regular part of the velocity autocorrelation function.[10] The Laplace transform of $\Delta V(t)$ is related to the irreducible memory function through

$$\Delta \tilde{V}(s) = \int_0^\infty dt e^{-st} \Delta V(t) = \lim_{q \to 0} \frac{\tilde{M}_S^{\text{irr}}(q,s)}{1 + \tilde{M}_S^{\text{irr}}(q,s)}, \tag{49}$$

where $\tilde{M}_S^{\text{irr}}(q,s)$ is the Laplace transform of $M_S^{\text{irr}}(q,t)$. The initially linear increase of $W(t)$ with slope D_S^S is followed by a sublinear regime that originates from the retarding influence of the cage of neighboring particles. At long times, $W(t)$ again becomes linear in t with a slope equal to the long-time self-diffusion coefficient $D_S^L < D_S^S$. The coefficient D_S^L follows from

$$D_S^L = \lim_{t\to\infty} \frac{W(t)}{t} = \frac{D_S^S}{1 + \tilde{M}_S^{\text{irr}}(q\to 0, s\to 0)}. \tag{50}$$

Alternatively, $W(t)$ and its long-time slope D_S^L can be determined directly from $G(q,t)$ via the extrapolation,

$$W(t) = -\lim_{q\to 0} \frac{\log G(q,t)}{q^2}. \tag{51}$$

Equations (40)–(47) constitute a self-consistent set of equations determining $S(q,t)$, $G(q,t)$, $\Delta\eta(t)$, and hence the related quantities η, $\eta'(\omega)$, $\eta''(\omega)$, $W(t)$, and D_S^L. The only input is the static structure factor $S(q)$ which can be calculated independently for a given pair potential using integral equation schemes or computer simulations.[10,56] An important feature of the coupled MCT equations with nonlinear feedback is that they predict an (idealized) glass transition scenario where long-time diffusion ceases and the zero-shear viscosity diverges. Within MCT, η diverges not at random close packing as η'_∞ does, but at a somewhat smaller volume fraction corresponding to the glass transition point. Recent experimental studies on hard sphere suspensions strongly support this scenario.[33–38]

IV. MCT LIMITING BEHAVIOR AND HYDRODYNAMIC RESCALING

Having established the basic MCT equations, we analyze next the asymptotic behavior of the MCT viscoelastic response functions for hard sphere dispersions ignoring HI. The neglect of HI in the equations presented above cannot be justified for actual hard sphere dispersions due to the strong near-field HI acting between nearly touching spheres. However, the MCT calculations of rheological and diffusional properties without many-body HI are important to assess the accuracy of the treatment of many-body direct interactions. Moreover, Brownian dynamics simulations are concerned generally with just direct potential interactions on the colloidal dynamics because of the difficulty to incorporate HI,[66] and to provide a useful check of the theoretical results.

From a short-time analysis of Eq. (40) for hard sphere colloids in the fluid regime, we obtain

$$\frac{\tau_a \Delta\eta(t)}{\eta_0} \approx \frac{9}{5}\Phi^2 \sqrt{\frac{2}{\pi}} g(2a^+)^2 \left(\frac{t}{\tau_a}\right)^{-1/2}, \tag{52}$$

provided that $t \ll \tau_a$. Correspondingly, the high-frequency behavior of the MCT moduli $G'(\omega)$ and $G''(\omega)$ differs from the exact result in Eqs. (20) and (21) only by a factor of $g(2a^+)/2$. Another limiting case which can be treated analytically in MCT is the asymptotic long-time behavior of $\Delta\eta(t)$ for a dilute hard sphere system without HI. Using Eq. (40) and noting that $dS(y)/dy = 24\Phi j_2(y)/y + \mathcal{O}(\Phi^2)$, where $y = 2ka$ and j_2 denotes the spherical Bessel function of the order of 2, we obtain in MCT the relaxation function to leading order in Φ:

$$\frac{\tau_a \Delta\eta(t)}{\eta_0} \approx \frac{36}{5\pi}\Phi^2 \int_0^\infty dy\, y^2 j_2(y)^2 e^{-y^2 t/(2\tau_a)} + \mathcal{O}(\Phi^3). \tag{53}$$

Since $j_2(y) \approx y^2/15$ for small y, we readily obtain the long-time form of the normalized shear relaxation function to leading, i.e., quadratic, order in Φ:

$$\frac{\tau_a \Delta\eta(t)}{\eta_0} \approx f_\infty \Phi^2 \sqrt{\frac{2}{\pi}} \left(\frac{t}{\tau_a}\right)^{-7/2}, \tag{54}$$

which is valid when $t \gg \tau_a$. In MCT, the prefactor is given by $f_\infty = 36/75 = 0.48$. The long-time behavior of the exact expression for $\Delta\eta(t)$ obtained in Ref. 46 differs from Eq. (54) only in the somewhat larger prefactor $f_\infty = 2/3 \approx 0.67$. While not reproducing accurately the prefactors of the exact short-time and long-time forms of $\Delta\eta(t)$, the MCT is at least qualitatively correct in predicting the exact asymptotic t dependence.

In performing the time integral of Eq. (53), we obtain the hard sphere MCT result,

$$\frac{\Delta\eta}{\eta_0} = f\Phi^2 + \mathcal{O}(\Phi^3), \tag{55}$$

for the thermodynamic part of the viscosity, with $f = 36/25 = 1.44$. For comparison, the exact result is Eq. (55) with the prefactor determined as $f = 12/5 = 2.4$.[46]

We proceed now to a discussion of the high frequency behavior of $\eta(\omega)$ for a model dispersion of charge-stabilized colloidal particles ignoring HI. The effective pair potential between two spherical particles is assumed to consist of a (masked) hard-core part with radius a, and of a long-range screened Coulomb part $u_{el}(r)$ which for $r > 2a$ is

$$\frac{u_{el}(r)}{k_B T} = 2Ka\frac{e^{-\kappa(r-2a)}}{r}. \tag{56}$$

Here, K is a dimensionless coupling parameter given by

$$K = \frac{L_B}{2a}\left(\frac{Z}{1+\kappa a}\right)^2, \tag{57}$$

where $L_B = e^2/(\epsilon k_B T)$ is the Bjerrum length for a suspending fluid of dielectric constant ϵ; in addition, Z is the effective charge number of a colloidal particle in units of the elementary charge e. The screening parameter κ is given by $\kappa^2 = 4\pi L_B[n|Z| + 2n_s] = \kappa_c^2 + \kappa_s^2$ where n_s is the number density of a possibly added 1-1 electrolyte. We note that κ comprises a contribution κ_c due to counterions, which are assumed to be monovalent, and a second contribution κ_s arising from the added electrolyte. Equation (57) is a good approximation of the effective pair potential of strongly charged particles, where the effective charge Z accounts for nonlinear screening effects.[10,67]

For charge-stabilized systems, G'_∞ exists even in the absence of HI and the large-ω behavior of $\eta''(\omega)$ is given according to Eq. (17) by

$$\frac{\eta''(\omega)}{\eta_0} \approx \frac{\tau_a}{\eta_0} G'_\infty (\omega\tau_a)^{-1}, \quad \omega\tau_a \gg 1, \tag{58}$$

with a regular ω^{-1} decay, different from the $\omega^{-1/2}$ decay for colloidal hard spheres. The MCT result for G'_∞ without HI is given by

J. Chem. Phys., Vol. 111, No. 18, 8 November 1999

Viscoelasticity of colloidal dispersions   8729

$$\frac{\tau_a}{\eta_0} G'_\infty = \frac{1}{80\pi} \int_0^\infty dy \left[\frac{y^2}{S(y)} \frac{d}{dy} S(y) \right]^2, \tag{59}$$

with $y = 2ka$. Since the singular hard core potential is masked by the strong electrostatic repulsion such that $g(r)$ behaves smoothly at distances r, we can employ Parseval's theorem and rewrite Eq. (59) as

$$\frac{\tau_a}{\eta_0} G'_\infty = -\frac{18}{5} \Phi^2 \int_0^\infty dx\, g(x) \frac{d}{dx} \left[x^4 \frac{d}{dx} c(x) \right], \tag{60}$$

with $x = r/(2a)$ and $c(x)$ denoting the direct correlation function. This MCT result for G'_∞ should be compared with the exact expression[40,68]

$$\frac{\tau_a}{\eta_0} G'_\infty = \frac{18}{5} \Phi^2 \int_0^\infty dx\, g(x) \frac{d}{dx} \left[x^4 \frac{d}{dx} \frac{u_{el}(x)}{k_B T} \right]. \tag{61}$$

Quite remarkably, the MCT result for G'_∞ becomes exact when $c(x)$ is approximated by $c(x) \approx -u_{el}(x)/(k_B T)$ for distances x with $g(x) \neq 0$. This well-established approximation for $c(x)$ is known in the literature as the rescaled mean spherical approximation (RMSA).[10]

It is also possible to deduce the large-ω behavior of $\eta'(\omega)$ from the large-q asymptotic behavior of $S(q)$. In RMSA, $S(q) - 1 \approx \mathcal{O}(q^{-3})$ for $q \to \infty$ since $g(2a^+) = 0$ in contrast to a hard sphere colloidal fluid where $S(q) - 1 \approx \mathcal{O}(q^{-2})$. This large-$q$ behavior gives rise to $\eta'(\omega) - \eta'_\infty$ decaying like $(\omega\tau_a)^{-3/2}$ for $\omega \to \infty$. Using the RMSA to calculate the static input $S(q)$ for the MCT equations, we will discuss in detail the frequency dependence of $\eta(\omega)$ in Sec. V.

In the MCT equations shown in Sec. III, we have so far not included the effect of HI. For concentrated hard sphere dispersions, one needs to account for many-body HI. Theories of diffusion and viscoelasticity which incorporate many-body HI exactly have not been developed to date, although many approximate theories of a varying degree of accuracy exist. For hard sphere dispersions we will employ a simple semi-empirical hydrodynamic rescaling procedure similar to that proposed by Medina-Noyola[43] and developed in more detail by Brady.[16,17] This rescaling procedure derives from the assumption that the diffusional and rheological transport properties with HI can be factorized into a hydrodynamic part, given by the corresponding short-time transport property with HI included, and a purely structural part without HI. In other words, it is assumed that the memory function contribution to the transport property is determined by structural effects only and not by HI.[69] To determine the structural part, we employ the MCT according to Sec. III, i.e., we use

$$W(t) \approx \left(\frac{D_S^S}{D_0} \right) W(t)^{MCT}, \tag{62}$$

corresponding to

$$D_S^L \approx \left(\frac{D_S^S}{D_0} \right) D_S^{L,MCT}. \tag{63}$$

Furthermore, $\Delta \eta(t)$ with HI is approximated by

$$\Delta \eta(t) \approx \left(\frac{\eta'_\infty}{\eta_0} \right) \Delta \eta^{MCT}(t), \tag{64}$$

with η determined from Eq. (23), and

$$D_C^L(q_m) \approx H(q_m) D_C^{L,MCT}(qm). \tag{65}$$

Here, the transport properties $W^{MCT}(t)$, $D_S^{L,MCT}$, and $\Delta \eta^{MCT}(t)$ without HI are calculated using the MCT expressions, Eqs. (51), (50), and (40), respectively. The long-time collective diffusion coefficient $D_C^{L,MCT}$ in Eq. (65) is calculated from the MCT-$S(q,t)$ without HI by extrapolating to the large-t regime according to [cf. Eq. (4)]

$$D_C^L(q_m) = -\frac{1}{q_m^2} \lim_{t \to \infty} \frac{\partial}{\partial t} \log S(q_m, t). \tag{66}$$

In Eq. (65), $H(q_m)$ is the so-called hydrodynamic function evaluated at wave number q_m where the principal peak of $S(q)$ occurs. Without HI it reduces to $H(q) = 1$. The factor $H(q_m)$ in Eq. (65) arises from the ratio of the short-time self-diffusion coefficient with HI, $D_C^S(q) = D_0 H(q)/S(q)$, to that without HI, i.e., $D_0/S(q)$ [cf. Eq. (41)]. We point out that the rescaling procedure in Eq. (63) is originally that of Medina-Noyola,[43] while Brady,[16] using a different justification for the factorization, also considered the viscosity. Neither of them, however, addressed rescaling of collective diffusion as proposed in Eq. (65). The hydrodynamic rescaling in Eq. (64) does not change the time dependence of $\Delta \eta(t)$. As a consequence, the hydrodynamically rescaled reduced dynamic viscosities $R(\omega)$ and $I(\omega)$ remain the same as without HI.

The hydrodynamic rescaling procedure in Eqs. (62)–(65) for colloidal hard spheres is semi-empirical and does not reproduce the known exact dilute limits of the long-time transport coefficients. Moreover, Eq. (64) does not recover a finite G'_∞ in the limit of $\omega \to \infty$, i.e., the exact short-time behavior of $\Delta \eta(t)$ is not reproduced. Notice that Eq. (62) gives the exact short-time form of $W(t)$. For the important case of concentrated dispersions, however, we will show in Sec. V that the hydrodynamic rescaling procedure leads to good agreement with experimental data, provided the Φ dependence of the MCT long-time transport properties without HI are renormalized with respect to the glass transition concentration (discussed below). To make quantitative comparisons with experimental hard sphere data using the rescaling procedure in Eqs. (62)–(65), we require the short-time transport coefficients $D_S^S(\Phi)$, η'_∞, and $H(q_m; \Phi)$ as input. For $\eta'_\infty(\Phi)$, we use the semi-empirical formula quoted in Eq. (24). For $D_S^S(\Phi)$, we employ an additional semi-empirical formula,

$$\frac{D_S^S(\Phi)}{D_0} = (1 - 1.56\Phi)(1 - 0.27\Phi), \tag{67}$$

suggested by Lionberger and Russel.[47] This expression conforms to the rigorous dilute limit $D_S^S/D_0 = 1 - 1.83\Phi$, with D_S^S vanishing at random close packing $\Phi = 0.64$.

We will demonstrate, by comparing with lattice-Boltzmann computer simulation data and experimental data of $H(q)$ by Segrè et al.,[70] that $H(q_m)$ is well represented by the form

$$H(q_m) = 1 - 1.35\Phi, \qquad (68)$$

up to the hard sphere freezing transition at $\Phi \approx 0.49$. This result unexpectedly conforms also to the exact numerical value in the dilute limit, which was determined by us using the exact two-body form of $\mathbf{D}_{ij}(\mathbf{R}^N)$.[13]

The hard sphere static structure factor, which is required as input for the MCT equations, is calculated according to the Verlet–Weiss correction of the Percus–Yevick (PY) $S(q)$.[56] The (idealized) MCT glass transition for this particular choice of $S(q)$ occurs at $\Phi = 0.525$,[21,33,71] where D_S^L vanishes. The caging of particles is, however, overestimated in MCT, leading to a glass transition concentration which is too low compared to experiments.[21,33–35,38,71] While the MCT does not predict an exact glass transition concentration, it does reproduce the special features of the colloidal hard sphere glass transition scenario. We therefore follow Götze and co-workers[21,33,38,64] and renormalize the concentration dependence of the MCT-calculated quantities (and only these), according to

$$\Phi \rightarrow \Phi \frac{\Phi_g}{0.525}, \qquad (69)$$

with the concentration Φ_g determined such that the MCT result for $D_S^L(\Phi)$ agrees well with BD data of D_S^L at high concentrations. This density renormalization yields $\Phi_g = 0.62$. A similar fit of the MCT predictions for D_S^L of atomic hard spheres to molecular dynamics data resulted in $\Phi_g = 0.60$.[71]

Contrary to hard sphere dispersions in which near-field lubrication forces are important, the dynamics of charged colloidal spheres is influenced only by the far-field part of the HI. There is no obvious reason to expect that the hydrodynamic rescaling relations in Eqs. (62)–(65) should apply for charge-stabilized colloids. In this context it should be noted that, while charge-stabilized fluid systems are usually dilute from a hydrodynamic point of view, they are effectively concentrated as far as the strong structural correlations are concerned [as measured, e.g., by Φ_{eff} introduced in Eq. (28) ff.]. Consider, e.g., the case of the self-diffusion of charged colloidal particles at low salinity, i.e., when $\kappa_s \ll \kappa_c$. For this case, a nonlinear Φ dependence of the form,

$$\frac{D_S^S(\Phi)}{D_0} = 1 - 2.5\Phi^{4/3}, \qquad (70)$$

has been predicted provided that $\Phi \lesssim 0.05$ and provided that electroviscous effects arising from the mobility of the counterion clouds are negligibly small.[10,53] The Φ dependence of D_S^S according to Eq. (70) has been qualitatively confirmed by recent dynamic light scattering experiments.[72] If the scaling relation in Eq. (63) for D_S^L would also hold for charged particles, then the ordering relation $D_S^L < (D_S^L)_{wo}$ should generally be valid, with $(D_S^L)_{wo}$ denoting the long-time self-diffusion coefficient in the absence of HI. In other words,

there would be a hydrodynamic de-enhancement of long-time diffusion for both uncharged and charged colloidal particles.

However, using a (not fully self-consistent) simplified solution of the MCT equations for charged spheres with the leading far-field HI included, it was observed that far-field HI leads instead to enlargement of D_S^L.[39] This finding has been corroborated by an exact low-density result for the D_S^L of the effective hard sphere system discussed in the final part of Sec. II. For the effective hard sphere system the long-time self diffusion coefficient is given in the dilute limit by

$$\frac{D_S^L}{D_0} = 1 - \Phi\left[2X^3 - \frac{33}{16}X^2 + \frac{567}{2560}X + \mathcal{O}(1)\right], \qquad (71)$$

with $X = b/a$.[39,73] For $X \gtrsim 3$, it follows from Eq. (71) that $D_S^L/D_0 > (D_S^L/D_0)_{wo} = 1 - 2\Phi X^3$. The hydrodynamic contributions in Eq. (71) proportional to X^2 and X are due to the leading Oseen term. The hydrodynamic enhancement of D_S^L due to prevailing far-field HI has been observed very recently in experiments and in BD simulations on quasi-two-dimensional superparamagnetic colloids with long-range dipolar magnetic forces,[74] and in de-ionized charge-stabilized dispersions.[75] The present discussion of long-time self-diffusion is meant to illustrate the qualitatively different dynamic behavior of colloidal hard spheres and of particle suspensions with long-range repulsive forces.

Another short-time feature that illustrates the qualitatively different behavior of hard sphere colloids and of charge-stabilized suspensions is the density dependence of the hydrodynamic function $H(q)$. One might expect that HI always leads to a slowing down of the particle density relaxation such that $H(q) < 1$ should hold at all wave numbers q. However, both experiments[76–78] and theoretical[10,39] calculations dealing with charged colloidal particles show that $H(q)$ can exceed 1 for values of q around q_m, and that the peak value $H(q_m)$ of $H(q)$ increases with increasing Φ. This behavior differs from that of hard spheres where $H(q_m)$ never exceeds unity and decreases (linearly up to freezing) with increasing Φ [cf. Eq. (68)]. Indeed, from our numerical calculations of $H(q)$ for de-ionized, i.e., salt-free, aqueous colloids of highly charged particles with effective charge number $Z = 500$ and radius $a = 50$ nm, in which the full two-body HI are accounted for, we find that $H(q_m)$ is, overall, well parametrized by the nonanalytic form,

$$H(q_m) \approx 1 + p\Phi^{0.4}, \qquad (72)$$

with $p = 1.5$ for all volume fractions in the extended range $\Phi \in (0,0.1)$ (cf. Sec. V). The exponent 0.4, in particular, is found to be independent of Z as long as the physical hard core remains completely masked. On the other hand, the prefactor p decreases with decreasing Z for a fixed particle radius. For example, $p = 1.5$, 1.35, and 1.12 for $Z = 500$, 400, and 300, respectively. Experimental results for the hydrodynamic function of suspensions of highly charged particles have been reported recently by Härtl and co-workers.[78] The measurements reveal pronounced oscillations in $H(q)$ even at volume fractions as low as 10^{-4}, in excellent agreement with the theoretical predictions of Nägele and Baur.[39]

Values of $H(q_m)$ larger than 1 are observed whenever the leading contribution of the far-field part $\mathbf{D}_{ij}(\mathbf{R}^N)$ $\approx D_0[\delta_{ij}\mathbf{1}+(1-\delta_{ij})\mathbf{O}(\mathbf{R}_i-\mathbf{R}_j)]$ of the diffusivity tensor dominates. Here,

$$\mathbf{O}(\mathbf{r})=\frac{3}{4}\left(\frac{a}{r}\right)[\mathbf{1}+\hat{\mathbf{r}}\hat{\mathbf{r}}], \tag{73}$$

is the Oseen tensor and $\hat{\mathbf{r}}=\mathbf{r}/r$.[10,39] The Oseen contribution dominates in dilute suspensions of strongly repelling charged particles. Using the Oseen approximation for $\mathbf{D}_{ij}(\mathbf{R}^N)$, $H(q_m)$ is approximated by the integral,

$$H(q_m)=1+6\pi na\int_0^\infty drr[g(r)-1]\left\{j_0(q_mr)-\frac{j_1(q_mr)}{q_mr}\right\}. \tag{74}$$

Substituting $z=q_mr$ and noting that $q_m\bar{r}$ $=q_ma[4\pi/(3\Phi)]^{1/3}\approx 2\pi$ holds for de-ionized systems, we can rewrite Eq. (74) as

$$H(q_m)=1+a_m\Phi^{1/3}, \tag{75}$$

with an exponent 1/3 rather close to 0.4 and the prefactor,

$$a_m=\left(\frac{81}{32\pi^4}\right)^{1/3}\int_0^\infty dzz[g(z)-1]\left\{\frac{j_1(z)}{z}-j_0(z)\right\}. \tag{76}$$

Within the framework of the effective hard sphere model discussed in Sec. II, we could approximate the $g(r)$ of the charge-stabilized system by the radial distribution function $g_{\text{EHS}}(z;\Phi_{\text{eff}})$ of the EHS model, evaluated at the effective volume fraction $\Phi_{\text{eff}}=\pi/6$. However, for numerical simplicity we again use the low density form $g_{\text{EHS}}^{(0)}(r)=\Theta(r-2b)$ corresponding to $g_{\text{EHS}}^{(0)}(z)=\Theta(z-2\pi)$. The integral in Eq. (76) can then be performed analytically with the result,

$$a_m=\left(\frac{81}{32\pi^4}\right)^{1/3}\approx 0.3. \tag{77}$$

The very small value obtained for a_m in Eq. (77) and the slight underestimation of the exponent 0.4 is due to the very crude step function approximation used for the actual $g(r)$. The latter can exhibit strong oscillations with a large peak value $g(r_m)$ which increases with Φ. Whereas the Φ dependence of the peak position of the actual $g(r)$ is accounted for in the step function approximation, the Φ dependence of the peak height is completely disregarded. Nonetheless, our simplified calculation shows that the nonlinear Φ dependence of $H(q_m)$ can be qualitatively understood in terms of this simple model of effective hard spheres with Φ-dependent effective particle radius b.

A second physically more intuitive explanation for the occurrence of values of $H(q)>1$ is as follows: $H(q)$ can be regarded as a generalized (short-time) sedimentation coefficient of particles exposed to spatially periodic external forces aligned with $\hat{\mathbf{q}}$, and derived from a weak potential proportional to $\exp[-i\mathbf{q}\cdot\mathbf{r}]$.[79] For $q\approx q_m\approx 2\pi/r_m$, $S(q,t)$ relaxes mainly by the motion of neighboring particles in opposite directions. The motion of a particle induces a backflow of displaced fluid, which can support the antagonistic motion of another neighbouring particle a distance r_m apart, thus leading to $H(q)>1$. The backflow becomes effective typically when $r_m>4a$ and this holds for many charge-stabilized suspensions. In contrast, $r_m=2a$ for hard sphere dispersions, and the weak (far-field) backflow effect is then outweighed by near-field HI, which favors the motion of particle pairs in the same direction. In other words, a hard sphere particle tends to drag along a closely spaced particle together with a thin coating of solvent sticking to the surfaces of both particles. Therefore, hard sphere dispersions exhibit $H(q_m)<1$.

Results for the short-time and long-time transport coefficients of charged and uncharged colloidal particles are presented and discussed in Sec. V.

V. NUMERICAL RESULTS AND DISCUSSION

Here in Sec. V we present extensive numerical results for the (frequency dependent) viscosity and short- and long-time diffusional and viscoelastic transport properties introduced in Secs. II–IV. Both fluid hard sphere suspensions and de-ionized charge-stabilized suspensions are considered. Furthermore, we examine the general validity of the various generalized Stokes-Einstein relations.

The MCT equations were solved in discretized form on a uniform wave vector grid with grid points $q=i\Delta q$, where $\Delta q\approx q_m/34$, using the algorithm developed by Fuchs et al.[80] The equations are numerically integrated forward in time starting from the known short-time behavior. In this algorithm it is made sure that the memory equations [Eqs. (41) and (45)] are satisfied at each discrete time step. To capture the short-time divergence of the irreducible memory functions and of $\Delta\eta(t)$, the integrals in Eqs. (42), (46), and (40) are performed on an extended wave number grid by extrapolating $S(q,t)$ and $G(q,t)$ to large values of q.

The effective pair potential of charged particles is modeled by Eq. (56), which constitutes the repulsive part of the well-known (Derjaguin–Landau–Vervey–Overbeck) DLVO potential. We limit ourselves to studying a de-ionized suspension with $n_s=0$, i.e., a suspension where the ionic strength is determined only by the counterions so that the potential is of long range and the particles become strongly correlated even at small volume fractions. The system parameters employed for the charge-stabilized systems are given by $Z=500$ for the effective particle charge number, $a=50$ nm for the particle radius, and Bjerrum length L_B $=0.714$ nm. These parameters are typical, e.g., of aqueous dispersions of highly charged polystyrene spheres. The static hard sphere input $S(q)$ and $g(r)$ are calculated using the Verlet-Weiss corrected PY approximation. In all MCT calculations of hard sphere properties, the Φ renormalization according to Eq. (69) with $\Phi_g=0.62$ is used. The RMSA structure functions $S(q)$ and $g(r)$ are employed in the case of charge-stabilized dispersions. No Φ renormalization is used in our MCT calculations for charge-stabilized systems, since no experimental or computer simulation reference points for $\Phi_g(Z,\kappa)$ are known for systems with high particle charges. There is, however, experimental support for the presence of a glass transition scenario in charge-stabilized systems.[81]

To compare the numerical results for the hard sphere dispersions with experimental data, we employ the hydrody-
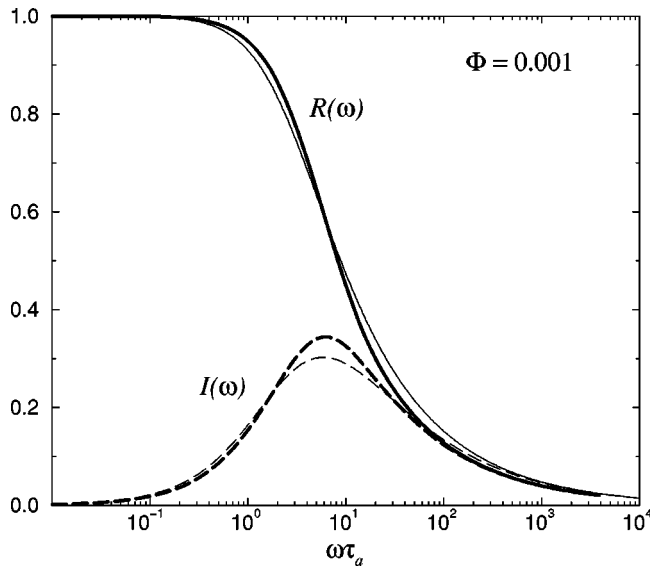
FIG. 1. Real part $R(\omega)$ and imaginary part $I(\omega)$ of the reduced dynamic viscosity vs $\omega\tau_a$ for a dilute hard sphere suspension with $\Phi = 0.001$ and HI ignored. Comparison between MCT results (thick lines) and exact low-density results (thin lines). The latter are reproduced from Ref. 46.
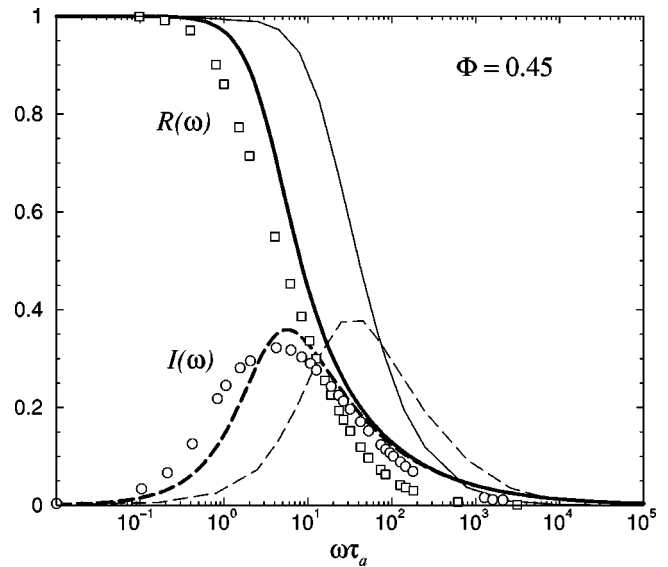
FIG. 2. Reduced dynamic viscosities $R(\omega)$ and $I(\omega)$ for a concentrated hard sphere suspension with $\Phi = 0.45$ and HI ignored. Thick lines: MCT results; open symbols: BD data of Heyes and Mitchell (Ref. 82); thin lines: nonequilibrium HNC closure scheme of Lionberger and Russel (Ref. 18).

namic short-time rescaling procedure described in Eqs. (63)–(65), with η'_∞, D_S^S, and $H(q_m)$ determined by Eqs. (24), (67), and (68), respectively. Since a corresponding hydrodynamic rescaling procedure for the long-time properties of charged colloidal particles is not available at this time, we neglect the effect of the far-field HI on diffusion and viscoelasticity. For de-ionized systems, however, we expect the transport properties to be only modestly influenced by HI. Our expectation is supported by exact low-density effective hard sphere model results for D_S^L [cf. Eq. (71)] and η,[46] and by (not fully self-consistent) MCT calculations of D_S^L,[39] which show only a modest hydrodynamic enhancement. Furthermore, the short-time properties of salt-free charge-stabilized dispersions vary also moderately as functions of Φ [cf. Eqs. (29), (70), and (72)]. To assess the accuracy of our numerical results, we compare them with both Brownian dynamics computer simulation results (without HI), and experimental data.

A. Viscoelasticity of uncharged and charged particles

In Fig. 1 we show the frequency dependence of the reduced dynamic viscosities $R(\omega)$ and $I(\omega)$ for a dilute hard sphere system without HI at $\Phi = 0.001$. The MCT results are compared with exact low-density results up to $\mathcal{O}(\Phi^2)$, obtained by Cichocki and Felderhof.[46] In their expressions for $R(\omega)$ and $I(\omega)$, we have corrected for a missing factor $(\omega\tau_a)^{1/2}$ multiplying the number 9 in the coefficient D given in Eq. (3.12) of Ref. 46. As can be seen in Fig. 1, the dynamic viscosity exhibits a broad spectrum of relaxation times. The maximum of the reduced imaginary part, $I(\omega)$, of $\eta(\omega)$ occurs in MCT at a reduced frequency $\omega_m\tau_a \approx 6.2$, rather close to the exact value $\omega_m\tau_a \approx 5.8$. We note that the approximations made in the MCT are aimed at describing the collective dynamic effects in highly correlated liquids.[21,33] There is therefore little reason to expect that the MCT will produce accurate results for the viscoelastic properties of di-

lute hard sphere dispersions. Nevertheless, we find that there is relatively good agreement between the MCT and the exact low-density results.

Figure 2 shows the MCT prediction for the reduced viscosities (without HI) for a concentrated hard sphere dispersion at $\Phi = 0.45$. The accuracy of our MCT results for $R(\omega)$ and $I(\omega)$ is assessed by comparison with BD data of Heyes and Mitchell.[82] The BD data have been obtained for a continuous pair potential $u(r)/(k_B T) = (2a/r)^{36}$, which closely approximates the singular hard core potential. The MCT results are seen to be in good qualitative agreement with the BD results. We have also included the results for the reduced viscosities obtained by Lionberger and Russel using a (hypernetted chain) HNC closure scheme for the shear-distorted nonequilibrium microstructure, also neglecting HI.[18] These results do not agree as well with the BD data as do those of the MCT, suggesting that the MCT provides a better approximation of the nonhydrodynamic excluded volume effects in colloidal hard sphere dispersions. An advantage of the nonequilibrium closure schemes developed by Lionberger and Russel is, however, that they can be used to predict the non-Newtonian rheological properties of sheared dispersions.[18,47]

Our MCT results for the Φ dependence of the zero-shear limiting suspension viscosity η of colloidal hard spheres with HI ignored are presented in Fig. 3. They are compared with the recent BD data of Strating.[66] As can be seen, the MCT predicts a strong increase in the viscosity with increasing volume fraction, in relatively good agreement with the BD data. It appears that the BD data are consistent with a viscosity which diverges at a volume fraction substantially lower than that of random close packing; recall that we have used a density renormalization such that the MCT viscosity diverges at a glass transition located at $\Phi = 0.62$. In principle, the glass transition is preempted by a fluid-solid transition at $\Phi \approx 0.49$. This phase transition can be suppressed in actual experiments by using dispersions with a slight size
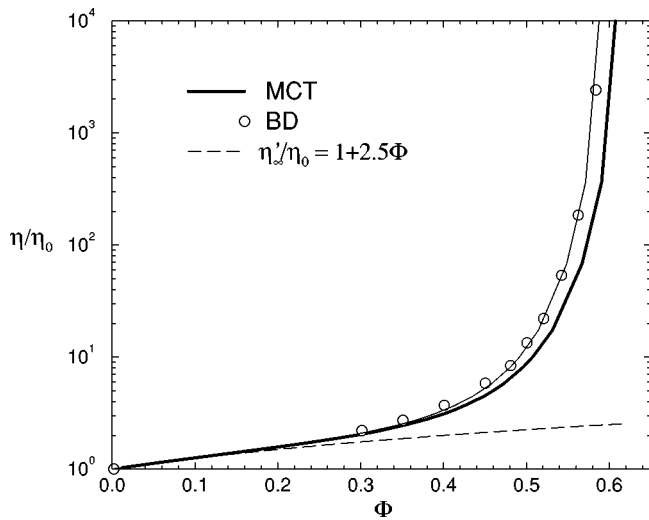
FIG. 3. Normalized shear viscosity without HI for colloidal hard spheres vs volume fraction Φ. Comparison between MCT results (thick solid line) and BD simulation data reproduced from Ref. 66. Thin solid line: MCT η/η_0 using $\Phi_g = 0.60$ instead of $\Phi_g = 0.62$. Dashed line: Einstein limiting result.
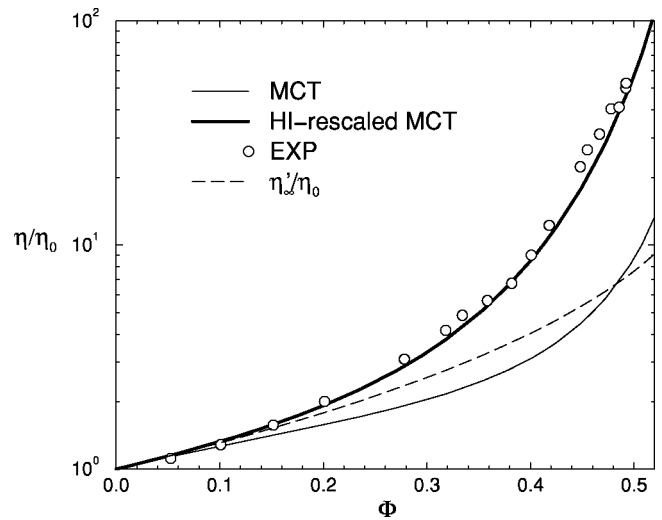

FIG. 4. Normalized shear viscosity with HI for hard sphere suspensions. Comparison between the HI-rescaled MCT result (thick solid line) and experimental data of Segrè et al. (Ref. 2) (open circles). Thin sold line: MCT result without HI; dashed line: η'_∞/η_0 according to Eq. (24).

polydispersity. The MCT η shown in Fig. 3 has been calculated from Eq. (23) with $\Delta\eta(t)$ determined according to Eq. (40). For the high frequency limiting viscosity the Einstein form $\eta'_\infty/\eta_0 = 1 + 2.5\Phi$ is used, which holds in the absence of HI (which was also done in the BD simulations). According to Fig. 3, the Einstein contribution to the potential part of η becomes negligible for $\Phi > 0.45$.

At this point, a few remarks are in order concerning the MCT renormalized value $\Phi_g = 0.62$ used throughout our calculations. This value was chosen to obtain optimal agreement of the MCT D_S^L with the corresponding hard sphere BD data at large Φ [cf. Fig. 13(b)]. There is, of course, a certain ambiguity in selecting this particular value of Φ_g. For instance, choosing a value $\Phi_g = 0.60$, a value somewhat closer to the experimentally determined glass transition concentration of 0.58,[34–37] would yield a MCT η in perfect agreement with the BD η shown in Fig. 3 (cf. the thin solid line). However, the BD D_S^L for concentrated hard spheres are then slightly underestimated. In general, it can be stated that overall good agreement between MCT and BD data for the diffusional and rheological properties is obtained for any choice of $\Phi_g \in (0.58 - 0.62)$.

So far we have disregarded the influence of HI on the (dynamic) viscosity. We account now for the influence of HI on η by using the approximate semi-empirical rescaling procedure given in Eq. (64) in conjunction with Eq. (23). For $\eta'_\infty(\Phi)$, we use the accurate expression in Eq. (24) which reduces to the Einstein form at small Φ. The HI-rescaled MCT result for $\eta(\Phi)$ is displayed in Fig. 4 and compared with experimental data of Segrè and co-workers[2] as well as with the MCT η without HI. Also shown is the Φ dependence of η'_∞ according to Eq. (24). We find that the rescaling of the MCT η brings the theory into good accord with the experimental data, at least on the semi-logarithmic scale used in Fig. 4. However, in absolute terms, the scaled MCT η can differ from the experimental data by as much as 25% for large Φ. Notice further that the experimental η is much

greater than the MCT η for $\Phi > 0.4$ when short-time rescaling is not used.

For hard sphere systems we analyze next the Φ dependence of the reduced dynamic viscosities. Recall that $R(\omega)$ and $I(\omega)$ remain unchanged when hydrodynamic rescaling according to Eq. (64) is applied. MCT results for concentrations $\Phi = 0.30$, 0.45, and 0.53 are presented in Fig. 5 as functions of $\omega\tau_a$, with the corresponding curves given from right to left. In the range of high volume fractions considered here, the frequency $\omega_m(\Phi)$ where the maximum of $I(\omega)$ occurs and the curves of $R(\omega)$ are monotonically shifting towards smaller frequencies with increasing Φ. However, $\omega_m(\Phi)$ is a nonmonotonic function when the whole Φ range of the fluid phase is considered. To make this quantitative we introduce the relaxation time $\tau_m(\Phi) = \omega_m^{-1}(\Phi)$ correspond-
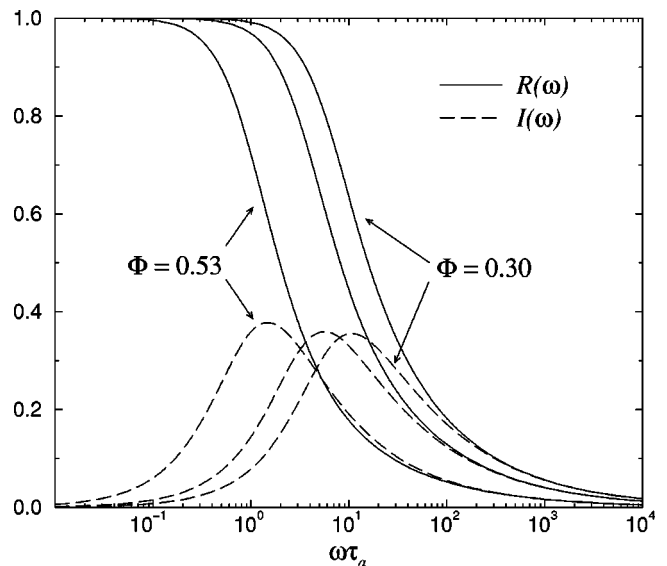

FIG. 5. Frequency dependence of reduced MCT dynamic viscosities $R(\omega)$ and $I(\omega)$ of colloidal hard spheres at $\Phi = 0.30$, 0.45, and 0.53 (from right to left).
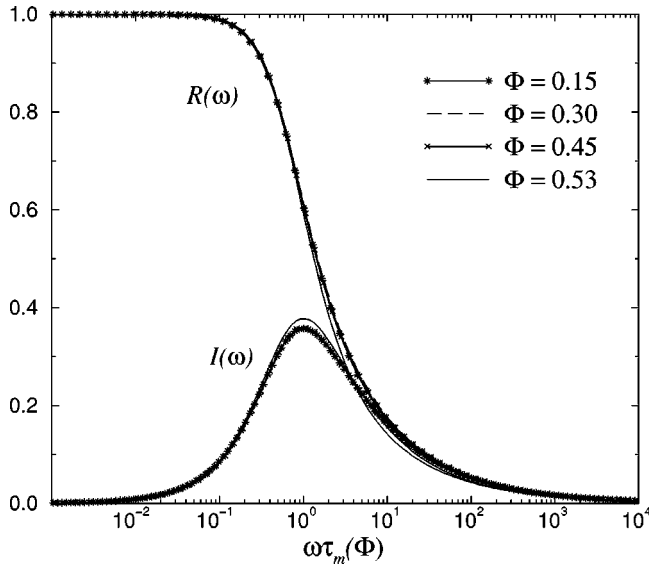
FIG. 6. MCT results for the reduced dynamic viscosities $R(\omega)$ and $I(\omega)$ vs $\omega\tau_m(\Phi)$ for hard sphere systems at varying volume fractions as labeled.
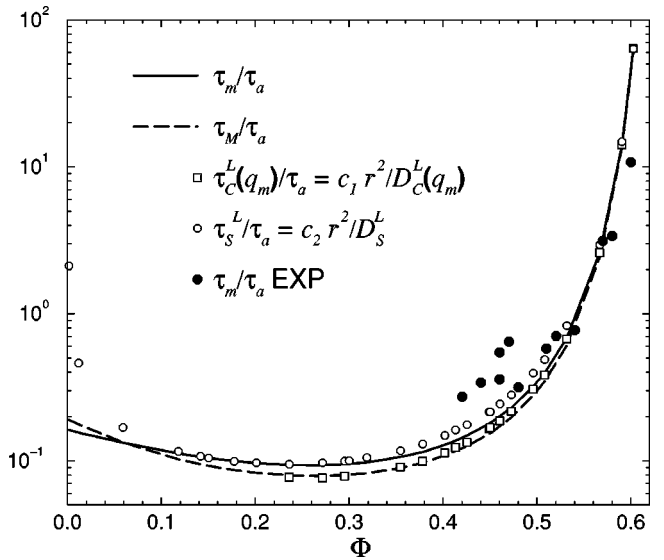

FIG. 7. Φ dependence of hard sphere normalized shear relaxation times $\tau_m(\Phi)$ and $\tau_M(\Phi)$ in comparison with normalized diffusion relaxation times $\tau_C^L(q_m;\Phi)$ and $\tau_S^L(\Phi)$. All quantities are calculated using MCT without HI, and compared with experimental data for τ_m of van der Werff *et al.* (Ref. 4).

ing to the frequency ω_m. The time $\tau_m(\Phi)$ can be regarded as an order of magnitude estimate of the mean (Maxwellian) relaxation time,[50]

$$\tau_M(\Phi) = \int_0^\infty dt\, t\, \frac{\Delta\eta(t)}{\Delta\eta} = \lim_{\omega\to 0}\frac{d}{d\omega}\left(\frac{\eta''(\omega)}{\Delta\eta}\right), \qquad (78)$$

related to the monotonically decaying shear relaxation function, with $\Delta\eta$ being the time integral of $\Delta\eta(t)$ according to Eq. (23). To leading order in Φ, τ_M is given exactly by $\tau_M/\tau_a = 2/9 \approx 0.22$ without HI, and by $\tau_M/\tau_a = 0.49$ when HI is considered.[50] For comparison, the small density MCT τ_M without HI follows from the time integral of Eq. (53) and with Eq. (55) as $\tau_M^{MCT}/\tau_a = 4/21 \approx 0.19$. The MCT τ_M is thus rather close to the exact value.

When the frequency dependence of $R(\omega)$ and $I(\omega)$ are scaled with respect to $\tau_m(\Phi)$, all curves essentially collapse on two single master curves. This is shown in Fig. 6 where MCT results for $R(\omega)$ and $I(\omega)$ are plotted versus $\omega\tau_m(\Phi)$ for various volume fractions as indicated. Similar findings have been obtained by van der Werff *et al.*[4] on sterically stabilized dispersions, and in the BD results of Heyes and Mitchell.[82]

The relaxation times $\tau_m(\Phi)$ and $\tau_M(\Phi)$ of hard spheres are nonmonotonic functions of Φ, with their respective minima occurring at $\Phi \approx 0.3$. The nonmonotonic dependence of τ_m and τ_M on Φ is shown in Fig. 7, where the MCT $\tau_m(\Phi)$ and $\tau_M(\Phi)$ curves without HI are included. At small Φ, the exact low-density result for τ_m is $\tau_m/\tau_a \approx 0.17$ without HI.[46] The corresponding MCT result is $\tau_m/\tau_a \approx 0.16$. It would be worthwhile to determine $\tau_m(\phi)$ and $\tau_M(\Phi)$ by computer simulations or by experiment in a density interval of $\Phi \approx 0.3$ to assess their nonmonotonic behavior. While not being identical, Fig. 7 reveals that both times have very similar Φ dependence. A physically intuitive explanation for the nonmonotonic behavior is as follows: the initial decrease of $\tau_M(\Phi)$ originates from the increasing number of collisions with increasing Φ, leading to faster relaxation of the shear

stress. At values $\Phi > 0.3$ it appears that particle caging becomes important, giving rise to a slower relaxation of the shear stress by particle diffusion with a further increase of Φ (cf. also the discussion for self diffusion in Ref. 83). In Fig. 7 we have also included experimental results for τ_m/τ_a obtained for hard sphere dispersions by van der Werff *et al.*[4] In their work, tabulated values for a so-called longest relaxation time $\tau_1(\Phi)$ are provided. By determining the maximum of $\eta''(\omega)$ according to Eq. (16) in Ref. 4, we find that τ_m is related to τ_1 by $\tau_m(\Phi) = \tau_1(\Phi)/1.176$.

It is interesting to compare the Φ dependence of τ_m and of τ_M with the Φ dependence of the characteristic diffusion times $\tau_C^L(q_m;\Phi)$ and $\tau_S^L(\Phi)$. The latter two quantities are related to long-time density relaxations at $q = q_m$ and to long-time self-diffusion, respectively, over a distance comparable to the geometric mean particle distance $\bar{r} = n^{-1/3} \propto \Phi^{-1/3}$. For the definition of these characteristic times consult the inset of Fig. 7. The constants $c_1 = 5.88 \times 10^{-3}/\tau_a$ and $c_2 = 9.09 \times 10^{-3}/\tau_a$ are conveniently chosen so that τ_C^L and τ_S^L are of comparable magnitude to τ_m, since we are only concerned here with their functional dependence on Φ.

The diffusion time $\tau_S^L(\Phi)$ diverges in the dilute limit, since $\bar{r} \to \infty$ and D_S^L is a bounded quantity. Notice further that the characteristic times τ_m, τ_M, $\tau_L^C(q_m)$, and τ_S^L diverge in a similar fashion when the glass transition concentration is approached.[33] The MCT results in Fig. 7 suggest that the times τ_C^L and τ_S^L, related to long-time collective and self-diffusion, respectively, behave similar to $\tau_M(\Phi)$ and $\tau_m(\Phi)$.

Having analyzed in detail the viscoelastic behavior of colloidal hard spheres, we investigate in the following the viscoelastic behavior of de-ionized suspensions of highly charged particles. Figure 8 contains MCT results without HI for the reduced dynamic viscosities of charged particles at volume fraction $\Phi = 0.04$. The remaining system parameters Z, $n_s = 0$, and L_B determining the pair potential in Eq. (57)
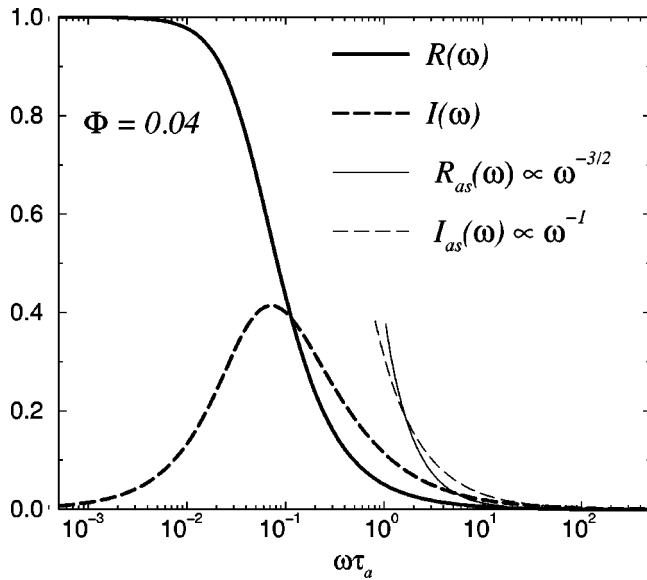
FIG. 8. MCT reduced dynamic viscosities $R(\omega)$ and $I(\omega)$ (thick lines) vs $\omega\tau_a$ for a de-ionized charge-stabilized system with $\Phi=0.04$, charge number $Z=500$, particle radius $a=50$ nm, and Bjerrum length $L_B=0.714$ nm. Thin lines: corresponding high frequency asymptotic forms $R_{as}(\omega)$ and $I_{as}(\omega)$.
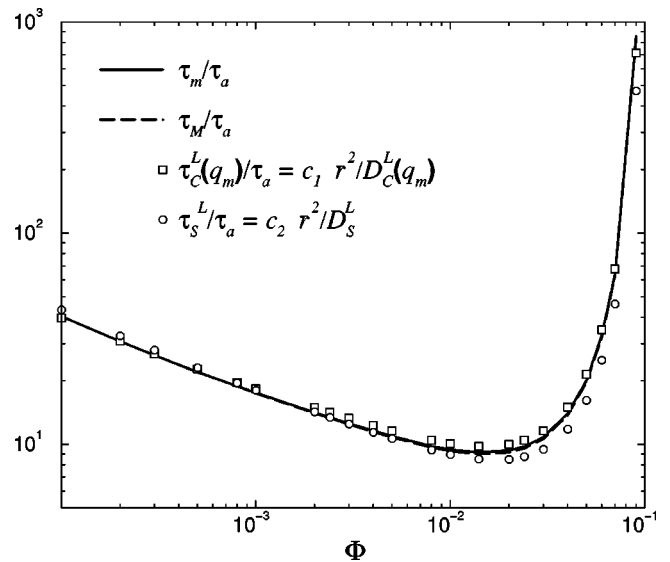

FIG. 9. Φ dependence of charged sphere normalized shear relaxation times $\tau_m(\Phi)$ and $\tau_M(\Phi)$ in comparison with normalized diffusion relaxation times $\tau_C^L(q_m;\Phi)$ and $\tau_S^L(\Phi)$, calculated using MCT without HI. Aside from Φ, all system parameters as in Fig. 8.

are chosen as those stated in the introductory part of Sec. V A. For this particular choice of potential parameters the MCT idealized glass transition occurs at $\Phi\approx0.1$, when the rescaled mean spherical approximation is used for $S(q)$. In Fig. 8, we also show the high frequency asymptotic forms $R_{as}(\omega)\propto(\omega\tau_a)^{-3/2}$ and $I_{as}(\omega)\propto(\omega\tau_a)^{-1}$ of $R(\omega)$ and $I(\omega)$. As discussed within the context of Eqs. (20), (21), (58), and (61), the high frequency asymptotes of charged particles are qualitatively different from those of hard spheres. The latter exhibit an asymptotic tail proportional to $(\omega)^{-1/2}$ when the HI are neglected. The intersection of $R(\omega)$ and $I(\omega)$ in Fig. 8 is caused by the faster asymptotic decay of $R(\omega)$.

The Φ dependence of the characteristic times $\tau_m(\Phi)$, $\tau_M(\Phi)$, $\tau_C^L(q_m;\Phi)$, and $\tau_S^L(\Phi)$ for charge-stabilized dispersions with the same coefficients c_1 and c_2 as those for the hard sphere suspensions is displayed in Fig. 9. The characteristic times diverge as the glass transition volume fraction is approached. All four characteristic times exhibit a similar density dependence as that observed also for the hard sphere dispersions. For the charge-stabilized system, the minimum of τ_m and τ_M at $\Phi\approx0.02$ is about two orders of magnitude larger than that for the hard sphere dispersions. Contrary to hard spheres, $\tau_M(\Phi)$ is now nearly identical with $\tau_m(\Phi)$. As seen in Fig. 10, $R(\omega)$ and $I(\omega)$ essentially collapse on the master curves when plotted versus $\omega\tau_m(\Phi)$. Note that the maximum of $I(\omega)$ yields a somewhat larger value for charged particles than for hard spheres (cf. Fig. 6).

B. Frequency-independent generalized Stokes-Einstein relations

Proceeding, we analyze next the validity of the short-time GSE relations in Eqs. (5) and (6), relating the high frequency viscosity η_∞' to the short-time self-diffusion coefficient D_S^S and to the short-time collective diffusion coeffi-

cient $D_C^S(q_m)=D_0 H(q_m)/S(q_m)$, respectively. Accurate expressions for the quantities involved in Eqs. (5) and (6) were provided earlier.

Consider first the Φ dependence of the hydrodynamic function $H(q_m)$. In Fig. 11(a), the hard sphere $H(q_m)$, evaluated according to Eq. (68), is plotted in comparison with experimental data of Segrè et al.[2] for concentrated dispersions (closed circles) and exact low-density calculations (crosses), with the two-body HI accounted for. The linear decrease of $H(q_m;\Phi)$, given by Eq. (68), holds up to high particle concentrations.

The corresponding density dependence of $H(q_m)$ for a charge-stabilized system, according to the nonanalytic para-
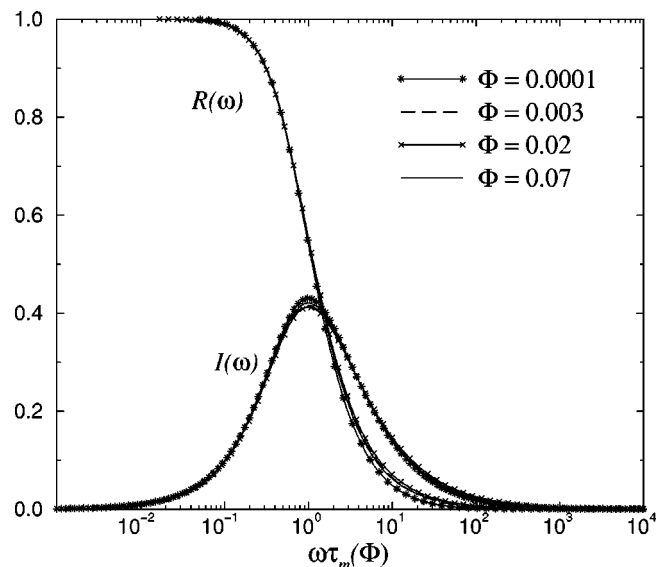

FIG. 10. MCT results for reduced dynamic viscosities $R(\omega)$ and $I(\omega)$ vs $\omega\tau_m(\Phi)$ for de-ionized charge-stabilized suspensions at varying volume fractions as labeled. All other parameters are the same as those in Fig. 8.
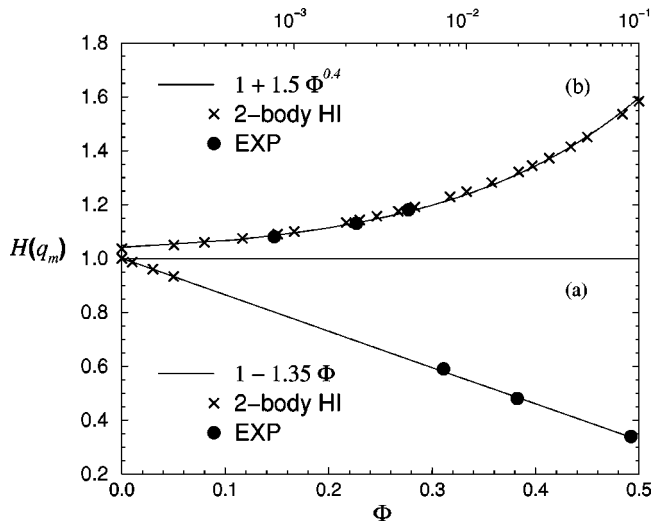
FIG. 11. (a) Hydrodynamic function $H(q_m)$ of colloidal hard spheres vs Φ. Solid line: parametric form Eq. (68); crosses: exact low density calculations; closed circles: experimental and computer simulational results taken from Ref. 70. (b) $H(q_m)$ of de-ionized charge-stabilized systems with $\Phi \in (0,0.1)$. The other parameters are the same as those in Fig. 8. Solid line: parametric form of Eq. (72); crosses: numerical low density results; closed circles: experimental results taken from Ref. 78.

metric form in Eq. (72) with $p=1.5$, is shown in Fig. 11(b). This parametric form provides a good description of the numerical results for $H(q_m)$, calculated with the full two-body HI included. As is seen, the calculated $H(q_m)$ is in good agreement with the experimental data of Härtl $et~al.$[78] on de-ionized suspensions of highly charged particles. The system parameters of the charge-stabilized suspensions studied by Härtl $et~al.$[78] are very similar to ours. Notice the qualitatively different Φ dependence for hard sphere dispersions and charge-stabilized systems.

In Fig. 12(a), we test the validity of the short-time GSE relations for hard spheres. Here, η'_∞, D_S^S, and $D_C^S(q_m)$ are determined from Eqs. (24), (67), and (68) with $S(q)$ calculated using the Verlet-Weiss correction of the PY approximation. According to Fig. 12(a), η'_∞ deviates from the reciprocal of D_S^S for all volume fractions. This finding is in agreement with the calculations of Beenakker for D_S^S.[84]

There is far better agreement between η'_∞ and the reciprocal of $D_C^S(q_m)$, the coefficients which are involved in the second short-time GSE in Eq. (6), at least for volume fractions up to $\Phi=0.4$. The calculations of $D_C^S(q_m)$ are in excellent agreement with the experimental data of Segrè $et~al.$,[70] which reflects the accuracy of Eq. (68) for $H(q_m)$ of hard sphere dispersions. This shows that the short-time GSE in Eq. (6), which is analogous to the long-time GSE discovered by Segrè $et~al.$,[2] provides a relatively good approximation for hard sphere dispersions. As seen, D_0/D_S^S according to Eq. (67) is in good agreement with experimental data of Segrè $et~al.$[70] (cf. also to Fig. 11).

Figure 12(b) contains the corresponding results for de-ionized charge-stabilized systems. Here, η'_∞ is approximated by Eqs. (28) and (29), respectively, which are practically equal to the Einstein form even up to the largest Φ of ~ 0.1. D_S^S is approximated by the nonanalytic form in Eq. (70), and $H(q_m)$ is determined from Eq. (72). The static structure fac-
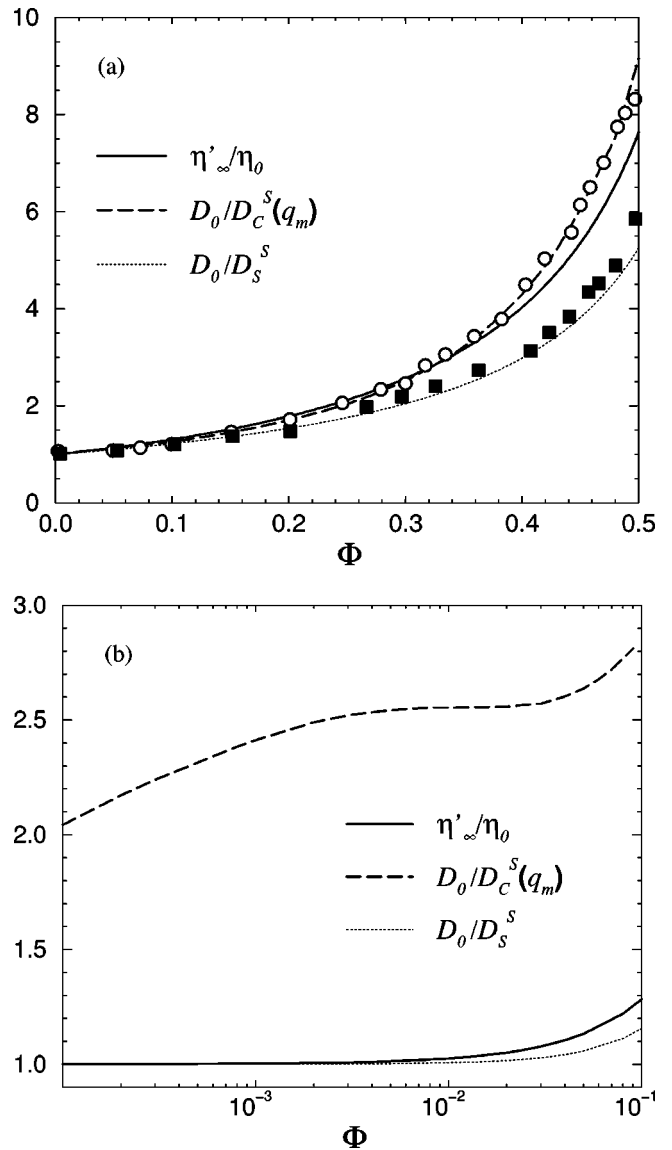

FIG. 12. (a) Calculated normalized high frequency limiting shear viscosity η'_∞/η_0, reciprocal short-time collective diffusion coefficient $D_0/D_C^S(q_m)$ at q_m, and reciprocal short-time self-diffusion coefficient D_0/D_S^S for hard sphere suspensions vs Φ. Open circles: Experimental $D_0/D_C^S(q_m)$; closed squares: experimental D_0/D_S^S reproduced from Ref. 70. (b) Corresponding short-time transport properties of charge-stabilized suspensions with system parameters, aside from Φ, the same as those in Fig. 8. η'_∞ is shown according to Eq. (28).

tor is obtained using the RMSA. As can be seen, both η'_∞/η_0 and D_0/D_S^S barely deviate from unity for concentrations up to $\Phi=0.03$. The deviation between the two quantities increases with increasing Φ, with η'_∞/η_0 being somewhat above D_0/D_S^S. This agrees qualitatively with the experimental measurements of Bergenholtz and co-workers on charge-stabilized dispersions at intermediate to high ionic strength.[7] Contrary to hard sphere dispersions, the GSE relation between η'_∞ and $D_C^S(q_m)$ is found to be strongly violated for the present case of de-ionized suspensions of highly charged particles.

In the following, we use the (rescaled) MCT to examine the two long-time GSE relations in Eqs. (1) and (3), relating η to the long-time self-diffusion coefficient D_S^L and to the
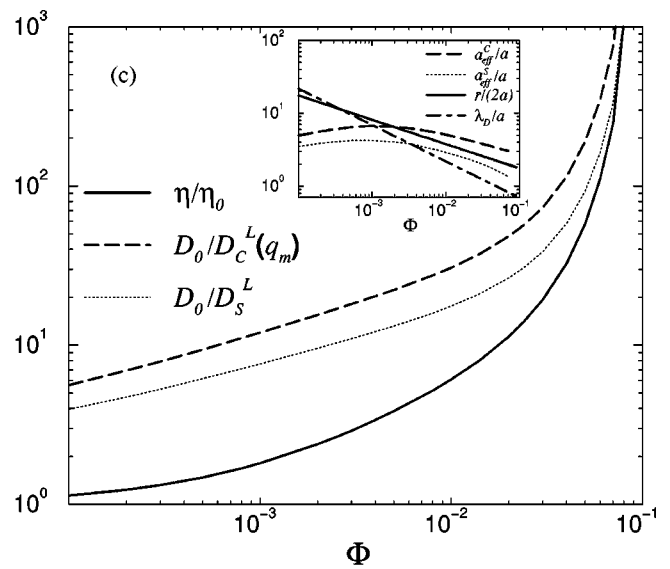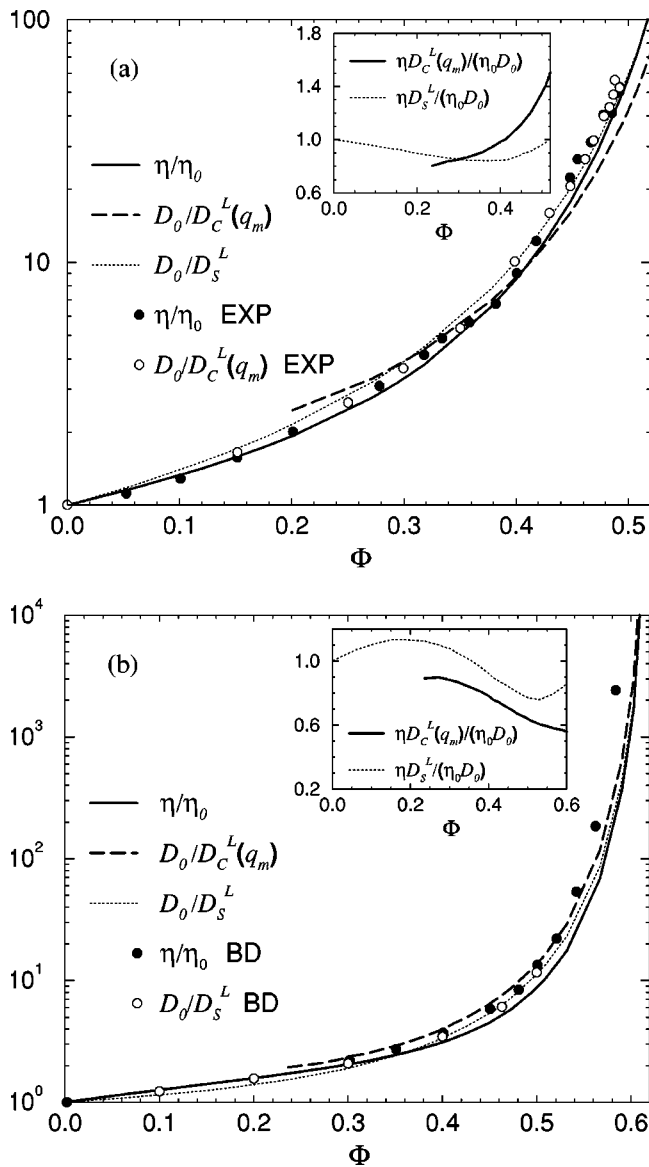
FIG. 13. (a) Experimental results for the normalized shear viscosity η/η_0 (closed circles) and for the normalized reciprocal long-time collective diffusion coefficient $D_0/D_C^L(q_m)$ (open circles) of hard sphere suspensions vs Φ reproduced from Ref. 2. The lines are the corresponding HI-rescaled MCT predictions, including the reciprocal long-time self-diffusion coefficient D_0/D_S^L. (b) BD results without HI for η/η_0 (closed circles, taken from Ref. 66) and for D_0/D_S^L (open circles, taken from Ref. 83) of hard sphere suspensions as functions of Φ. The lines are the corresponding MCT predictions without HI as labeled. (c) MCT results without HI for the normalized (reciprocal) long-time transport coefficients of charge-stabilized systems with system parameters, aside from Φ, the same as those in Fig. 8. Various definitions of effective radii are displayed in the inset.

long-time collective diffusion coefficient $D_C^L(q_m)$, respectively.

The HI-rescaled MCT hard sphere results for η/η_0, D_0/D_S^L, and $D_0/D_C^L(q_m)$ are displayed in Fig. 13(a), together with experimental data of Segrè et al.[2] for η and for $D_C^L(q_m)$. On the semi-logarithmic scale in Fig. 13(a), there is good agreement between η/η_0 and D_0/D_S^L. Close agreement between these two quantities was also observed experimentally by Imhof et al.,[12] while Segrè et al. found deviations at high particle concentrations.[2] The rescaled MCT predicts that η also very crudely obeys a GSE with $D_C^L(q_m)$. This MCT $D_C^L(q_m)$ agrees qualitatively with the data obtained by Segrè et al. for $\Phi \in (0.28-0.45)$. As we will argue below, $D_C^L(q_m)$ and hence the GSE in Eq. (3) cease to exist for hard spheres at small volume fractions.

The GSE relation between η and D_S^L has also been investigated theoretically for hard spheres by Lionberger and Russel[18] using the nonequilibrium HNC closure scheme with HI accounted for in two different ways. Their findings for the product of $\eta D_S^L/(\eta_0 D_0)$ vs Φ are qualitatively similar to

ours, in particular for the so-called discontinuous HI approximation used in their work.

To study the effect of the excluded volume interactions alone, we show the hard sphere MCT results without HI rescaling in Fig. 13(b). Also shown are Strating's BD data for η[66] and BD data for D_S^L obtained by Cichocki and Hinsen.[83] In comparing Fig. 13(b) with Fig. 13(a), the hydrodynamically induced enhancement of η and the more modest de-enhancement of D_S^L are clearly observed. Let us recall that the value $\Phi_g = 0.62$ in the MCT Φ renormalization was chosen so that the high density part of the BD data for D_S^L agrees well with the MCT D_S^L [cf. Fig. 13(b)]. As is seen in Fig. 13(b), the BD data for η/η_0 and D_0/D_S^L are in good agreement and in accord with the corresponding MCT results. The MCT results for D_0/D_S^L are seen to be somewhat closer to η/η_0 than the MCT results for $D_0/D_C^L(q_m)$.

Notice in Figs. 13(a) and 13(b) that $D_C^L(q_m)$ is shown only for densities $\Phi > 0.22$. For $\Phi \lesssim 0.22$, the MCT $S(q_m,t)$ ceases to be a purely exponentially decaying function at long times. The disappearance of the exponential mode of

$S(q_m, t)$ at smaller Φ is not an artifact of the MCT, but is corroborated by hard sphere calculations of $S(q_m, t)$ at intermediate concentrations based on the so-called contact-Enskog approximation.[85,86] It should be kept in mind that $S(q,t)$ shows, in general, an overall nonexponential time dependence. For example, for hard sphere suspensions to first order in Φ, an asymptotic long-time behavior of $S(q,t)$ proportional to $t^{-3/2} \exp[-q^2(D_0/2)t]$ is obtained from exact calculations at all wave numbers $q>0$.[85–87] The same algebraic-exponential long-time decay form of $S(q,t)$ is predicted in MCT, up to a somewhat different prefactor, both for dilute hard sphere suspensions and in the weak coupling limit. The coefficient $D_C^L(q_m)$ characterizes the long-time exponential decay of density fluctuation correlations linked to the average extension, $2\pi/q_m$, of a next-neighbor cage. This so-called collective mode should therefore only occur at concentrations that are large enough that caging effects are significantly strong. The occurrence of an exponential collective long-time mode in $S(q_m, t)$ at values $\Phi > 0.22$ is intimately related to the presence of an isolated satellite peak at the small frequency (i.e., small λ) side of the otherwise continuous spectral density $p_{q_m}(\lambda)$, related to $S(q_m, t)$ by $S(q_m, t)/S(q_m) = \int_0^\infty d\lambda \exp(-\lambda t) p_{q_m}(\lambda)$. A detailed analysis of the functional form of the MCT spectral density will be given elsewhere, since it is not central to the topic presented in this work.

Next, we examine whether the long-time GSEs are likely to hold independent of the pair potential. To this end, we apply the MCT to the dispersions of highly charged spheres for which the interaction potential is far from hard sphere like.

The MCT results for η/η_0, D_0/D_S^L, and $D_0/D_C^L(q_m)$ as functions of Φ are shown in Fig. 13(c) up to the glass transition volume fraction ($\Phi \approx 0.1$). Neither HI rescaling nor the Φ renormalization has been employed here for the reasons discussed in the introductory part of Sec. V.

According to the MCT, both long-time GSEs are violated for de-ionized systems. The deviations from the two GSEs are so strongly pronounced that it appears very unlikely that the inclusion of far-field HI effects will reestablish either of the two relations. A somewhat reassuring aspect of these MCT calculations is that they agree with the two freezing criteria proposed by Hansen and Verlet[88] and by Löwen et al.;[89] the former relates the volume fraction at which crystallization begins to $S(q_m) \approx 2.85$, whereas the latter is dynamic in nature in that it states that $D_S^L/D_0 \approx 0.1$ at the freezing volume fraction. At $\Phi \approx 2.4 \times 10^{-3}$ the RMSA $S(q_m) \approx 2.85$ corresponds indeed to $D_S^L/D_0 \approx 0.1$ in Fig. 13(c). Thus, according to the MCT calculations, these freezing criteria are consistent, revealing that for concentrations above $\Phi \approx 2.4 \times 10^{-3}$ these dispersions are in an undercooled liquid state.

For the charge-stabilized systems in this study, we can formally write $D_S^L = k_B T/(6\pi\eta a_{\text{eff}}^S)$ and $D_C^L(q_m) = k_B T/(6\pi\eta a_{\text{eff}}^C)$, which defines two effective (hydrodynamic) radii $a_{\text{eff}}^S > a$ and $a_{\text{eff}}^C > a$. Their Φ dependence is displayed in the inset of Fig. 13(c), and compared with the Φ dependence of $r_m \approx \bar{r} \propto \Phi^{-1/3}$ and the Debye screening length $\lambda_D = \kappa^{-1} \propto \Phi^{-1/2}$. Both effective radii a_{eff}^S and a_{eff}^C are non-

monotonic in Φ and hence cannot be expressed in terms of a single power law in Φ. Notice that $S(q_m) \approx 2.1$ for the smallest concentration $\Phi = 10^{-4}$ considered in Fig. 13(c).

C. Frequency-dependent generalized Stokes-Einstein relations

In the following we investigate the frequency dependent empirical GSE relation in Eq. (7) given by Mason and Weitz,[1,26] using the rescaled and unscaled MCT for hard sphere and charge-stabilized dispersions, respectively. As pointed out in Sec. I, this GSE conforms to the short-time GSE between η_∞' and D_S^S and the long-time GSE between η and D_S^L in the limit of $s \to \infty$ and $s \to 0$, respectively.

For hard sphere dispersions, we compare in Fig. 14(a) the Laplace-transformed normalized dynamic viscosity $\tilde{\eta}(s)/\eta_0 = \eta(i\omega)/\eta_0$ with the function $D_0/[s\tilde{D}(s)]$. Both quantities are computed using the HI-rescaling procedure of Eqs. (62) and (64), with η_∞' according to Eq. (24). The rescaling of the MCT results leads to good agreement in the low frequency regime, suggesting that the Mason and Weitz GSE is valid approximatively over an extended Φ range. It should be noted that $\tilde{\eta}(s)$ is a monotonically decreasing function of s since $\Delta\eta(t)$ is non-negative. The high- and low-s limits of the Mason and Weitz GSE are compatible with the monotonic decrease of $\tilde{\eta}(s)$, since $D_S^L < D_S^S$ is valid independent of the pair potential.

The MCT results for charged colloidal particles with HI neglected are shown in Fig. 14(b). As can be seen, the MCT predicts that the frequency dependent GSE is violated for charged colloidal particles, as was found also for the frequency independent long-time GSEs.

In the remainder of Sec. V, we analyze the frequency dependence of $\tilde{\eta}(s)$ and the Laplace-transformed diffusion function. For this we define the reduced quantities,

$$\Psi_\eta(s) = \frac{\tilde{\eta}(s) - \eta_\infty'}{\eta - \eta_\infty'}, \tag{79}$$

and

$$\Psi_D(s) = \frac{1/(s\tilde{D}(s)) - 1/D_S^S}{1/D_S^L - 1/D_S^S}, \tag{80}$$

associated with $\tilde{\eta}(s)$ and $1/[s\tilde{D}(s)]$. The functions $\Psi_\eta(s)$ and $\Psi_D(s)$ vary between 0 and 1. For fluids, they decay monotonically from 1 at $s=0$ to 0 for $s \to \infty$. Since the HI-rescaling procedure in Eqs. (62)–(65) does not affect the time dependence of $W^{\text{MCT}}(t)$ and $\Delta\eta(t)$, $\Psi_\eta(s)$ and $\Psi_D(s)$ remain unchanged with and without it.

Figures 15(a) and 15(b) show MCT results for $\Psi_\eta(s)$ and $\Psi_D(s)$ for colloidal hard spheres and charged spheres, respectively, as functions of the reduced frequency $s\tau_a$, and in the hard sphere case, for volume fractions up to $\Phi = 0.57$. We observe remarkably good agreement between $\Psi_\eta(s)$ and $\Psi_D(s)$ for hard spheres, but even better agreement results for de-ionized systems. For hard spheres, the agreement between $\Psi_\eta(s)$ and $\Psi_D(s)$ becomes good for concentrated systems with $\Phi > 0.2$, improving further with increasing Φ [cf. the inset of Fig. 15(a)]. Notice that charge-stabilized systems are effectively concentrated even for the
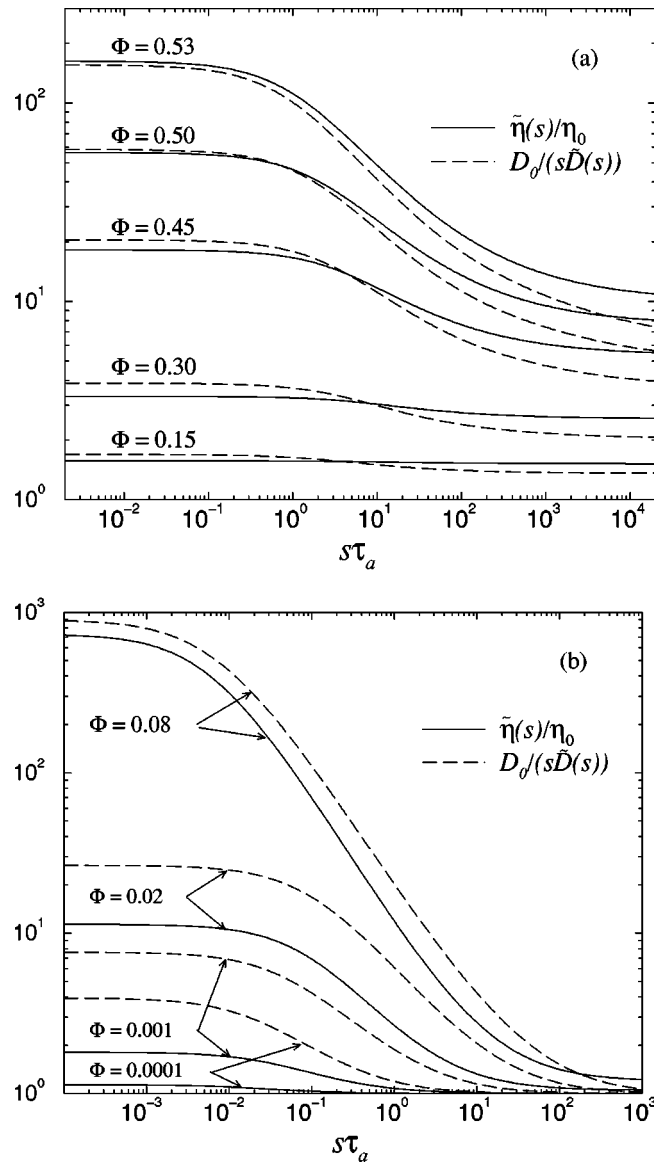
FIG. 14. (a) Comparison of Laplace-transformed normalized dynamic viscosity $\tilde{\eta}(s)/\eta_0$ (solid lines) with $D_0/[s\tilde{D}(s)]$ (dashed lines) vs $s\tau_a$ for hard sphere dispersions. Both quantities are calculated using the HI-rescaled MCT. The volume fractions are as labeled. (b) MCT results without HI for charge-stabilized systems with system parameters, aside from Φ, the same as those in Fig. 8.
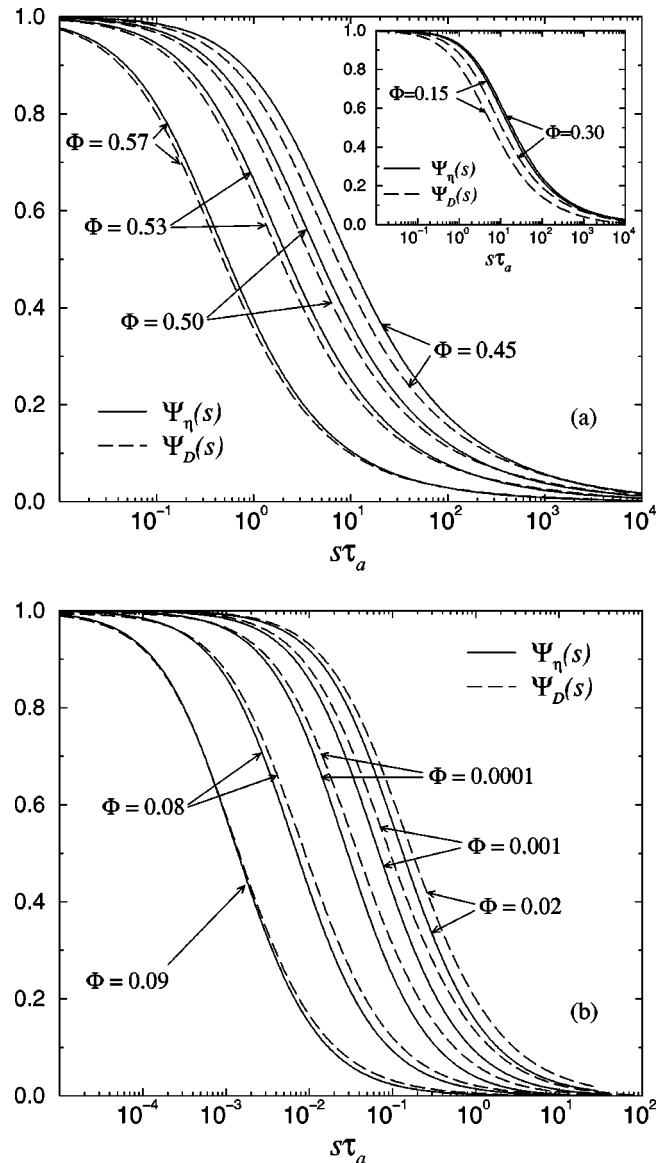
FIG. 15. (a) MCT hard sphere results for reduced dynamic quantities $\Psi_\eta(s)$ (solid lines) and $\Psi_D(s)$ (dashed lines) defined in Eqs. (79) and (80), respectively, as functions of $s\tau_a$. The volume fractions are as labeled. For clarity, results for $\Phi=0.15$ and 0.30 are shown in the inset. (b) Corresponding MCT results for charge-stabilized systems. The system parameters, aside from Φ, are the same as those in Fig. 8. The volume fractions are as labeled.

smallest physical volume fractions considered. Consequently, the MCT predicts the following frequency dependent GSE to provide a good approximation for both hard sphere and charged sphere dispersions:

$$\Psi_\eta(s) = \Psi_D(s). \tag{81}$$

Computer simulations or experiments can be used to decisively test this new finding.

VI. CONCLUDING REMARKS

We have examined in detail the linear viscoelastic properties and the diffusion of hard sphere and charge-stabilized dispersions of colloidal particles. Particular focus has been directed at evaluating the range of validity of several generalized Stokes-Einstein relations which have been proposed to

hold to various degrees of approximation for concentrated and highly correlated dispersions. In addition, this study has identified new extensions of them for short times and finite frequencies, which may prove useful for estimating linear viscoelastic properties from dynamic light scattering measurements, or vice versa.

The MCT results can be brought into accord with Brownian dynamics simulation data for the shear viscosity and long-time self-diffusion coefficient of hard spheres by renormalizing the volume fraction. Inclusion of a full accounting of HI in the MCT calculations is, as for any theory of concentrated suspensions, a daunting task that has not yet been accomplished. In this work for hard spheres we employ a simple hydrodynamic rescaling procedure. In this way the MCT results can be quantitatively compared with experi-

mental measurements of the frequency dependent viscosity and the long-time diffusion coefficients of hard sphere dispersions.

The MCT results suggest that a connection exists between the linear viscoelastic behavior and the self and cooperative particle motion in dispersions. The Maxwell relaxation time was found to be linked to appropriately normalized long-time diffusion coefficients irrespective of the nature of the interaction potential. Both short- and long-time versions of the frequency independent GSEs were found to hold approximately for hard spheres, whereas no such relation appears to be valid for dispersions of highly charged particles. A similar conclusion holds for the case of the frequency dependent GSE suggested in Ref. 1, whereas a modified version of this GSE should, according to our calculations, yield an improved frequency dependent GSE correlation for dispersions with strong concentration- or potential-induced interactions.

ACKNOWLEDGMENTS

[1] T. G. Mason and D. A. Weitz, Phys. Rev. Lett. **74**, 1250 (1995).
[2] P. N. Segrè, S. P. Meeker, P. N. Pusey, and W. C. K. Poon, Phys. Rev. Lett. **75**, 958 (1995).
[3] T. Shikata and D. S. Pearson, J. Rheol. **38**, 601 (1994).
[4] J. C. van der Werff, C. G. de Kruif, C. Blom, and J. Mellema, Phys. Rev. A **39**, 795 (1989).
[5] S.-E. Phan *et al.*, Phys. Rev. E **54**, 6633 (1996).
[6] N. J. Wagner and A. T. J. M. Woutersen, J. Fluid Mech. **278**, 267 (1994).
[7] J. Bergenholtz *et al.*, Phys. Rev. E **58**, R4088 (1998).
[8] W. B. Russel, D. A. Saville, and W. R. Schowalter, *Colloidal Dispersions* (Cambridge University Press, Cambridge, 1989).
[9] P. N. Pusey, in *Liquids, Freezing and Glass Transition*, edited by J.-P. Hansen, D. Levesque, and J. Zinn-Justin (North-Holland, Amsterdam, 1991), pp. 763–942.
[10] G. Nägele, Phys. Rep. **272**, 215 (1996).
[11] J. X. Zhu *et al.*, Phys. Rev. Lett. **68**, 2559 (1992).
[12] A. Imhof *et al.*, J. Chem. Phys. **100**, 2170 (1994).
[13] A. J. Banchio, J. Bergenholtz, and G. Nägele, Phys. Rev. Lett. **82**, 1792 (1999).
[14] M. M. Kops-Werkhoven and H. M. Fijnaut, J. Chem. Phys. **77**, 2242 (1982).
[15] A. van Blaaderen, J. Peetermans, G. Maret, and J. K. G. Dhont, J. Chem. Phys. **96**, 4591 (1992).
[16] J. F. Brady, J. Chem. Phys. **99**, 567 (1993).
[17] J. F. Brady, J. Fluid Mech. **272**, 109 (1994).
[18] R. A. Lionberger and W. B. Russel, J. Rheol. **41**, 399 (1997).
[19] D. L. Cebula, R. H. Ottewill, J. Ralston, and P. N. Pusey, J. Chem. Soc., Faraday Trans. 1 **77**, 2585 (1981).
[20] P. Licino and M. Delaye, J. Phys. (Paris) **49**, 975 (1988).
[21] For a review, see W. Götze, in Ref. 9.
[22] M. Fuchs, I. Hofacker, and A. Latz, Phys. Rev. A **45**, 898 (1992).
[23] R. Sigel *et al.* (unpublished).
[24] R. J. Phillips, J. F. Brady, and G. Bossis, Phys. Fluids **31**, 3462 (1988).
[25] A. J. C. Ladd, J. Chem. Phys. **93**, 3484 (1990).
[26] T. G. Mason, H. Gang, and D. A. Weitz, J. Mol. Struct. **383**, 180 (1996).
[27] J. Bosse, W. Götze, and M. Lücke, Phys. Rev. A **17**, 434 (1978).
[28] J. Bosse, W. Götze, and M. Lücke, Phys. Rev. A **17**, 447 (1978).
[29] L. Sjögren, Phys. Rev. A **22**, 2883 (1980).
[30] E. Leutheusser, Phys. Rev. A **29**, 2765 (1984).
[31] U. Bengtzelius, W. Götze, and A. Sjölander, J. Phys. C **17**, 5915 (1984).
[32] W. Götze and L. Sjögren, Z. Phys. B: Condens. Matter **65**, 415 (1987).
[33] For a review, see, for example, W. Götze and L. Sjögren, Rep. Prog. Phys. **55**, 241 (1992).
[34] W. van Megen and S. M. Underwood, Phys. Rev. E **49**, 4206 (1994).
[35] W. van Megen, Transp. Theory Stat. Phys. **24**, 1017 (1995).
[36] P. N. Pusey and W. van Megen, Phys. Rev. Lett. **59**, 2083 (1987).
[37] W. van Megen and P. N. Pusey, Phys. Rev. A **43**, 5429 (1991).
[38] W. Götze and L. Sjögren, Phys. Rev. A **43**, 5442 (1991).
[39] G. Nägele and P. Baur, Physica A **245**, 297 (1997).
[40] G. Nägele and J. Bergenholtz, J. Chem. Phys. **108**, 9893 (1998).
[41] G. Nägele and J. K. G. Dhont, J. Chem. Phys. **108**, 9566 (1998).
[42] G. Nägele, J. Bergenholtz, and J. K. G. Dhont, J. Chem. Phys. **110**, 7037 (1999).
[43] M. Medina-Noyola, Phys. Rev. Lett. **60**, 2705 (1988).
[44] M. Fuchs and M. R. Mayr, Phys. Rev. E (in press).
[45] G. K. Batchelor, J. Fluid Mech. **83**, 97 (1977).
[46] B. Cichocki and B. U. Felderhof, Phys. Rev. A **43**, 5405 (1991).
[47] R. A. Lionberger and W. B. Russel, J. Rheol. **38**, 1885 (1994).
[48] W. B. Russel and A. P. Gast, J. Chem. Phys. **84**, 1815 (1986).
[49] G. K. Batchelor and J. T. Green, J. Fluid Mech. **56**, 401 (1972).
[50] B. Cichocki and B. U. Felderhof, J. Chem. Phys. **101**, 7850 (1994).
[51] W. B. Russel, J. Chem. Soc., Faraday Trans. 2 **80**, 31 (1984).
[52] M. Watzlawek and G. Nägele, Physica A **235**, 56 (1997).
[53] M. Watzlawek and G. Nägele, Phys. Rev. E **56**, 1258 (1997).
[54] D. M. E. Thies-Weesie *et al.*, J. Colloid Interface Sci. **176**, 43 (1995).
[55] M. Watzlawek and G. Nägele, J. Colloid Interface Sci. **124**, 170 (1999).
[56] J.-P. Hansen and I. R. McDonald, *Theory of Simple Liquids*, 2nd ed. (Academic, New York, 1986).
[57] D. J. Jeffrey, Phys. Fluids A **4**, 16 (1992).
[58] S. Kim and S. J. Karrila, *Microhydrodynamics: Principles and Selected Applications*, Series in Chemical Engineering (Butterworth-Heinemann, Boston, 1991).
[59] D. R. Foss and J. F. Brady, J. Fluid. Mech. (submitted).
[60] D. R. Foss and J. F. Brady, J. Fluid. Mech. (submitted).
[61] T. Geszti, J. Phys. C **16**, 5805 (1983).
[62] R. Verberg, I. M. de Schepper, and E. G. D. Cohen, Phys. Rev. E **55**, 3143 (1997).
[63] I. M. de Schepper, H. E. Smorenburg, and E. G. D. Cohen, Phys. Rev. Lett. **70**, 2178 (1993).
[64] M. Fuchs, Transp. Theory Stat. Phys. **24**, 855 (1995).
[65] G. Szamel and H. Löwen, Phys. Rev. A **44**, 8215 (1991).
[66] P. Strating, Phys. Rev. E **59**, 2175 (1999).
[67] J. C. Crocker and D. A. Grier, Phys. Rev. Lett. **73**, 352 (1994).
[68] R. Zwanzig and R. D. Mountain, J. Chem. Phys. **43**, 4464 (1965).
[69] J. F. Brady, Curr. Opin. Colloid Interface Sci. **1**, 472 (1996).
[70] P. N. Segrè, O. P. Behrend, and P. N. Pusey, Phys. Rev. E **52**, 5070 (1995).
[71] J. L. Barrat, W. Götze, and A. Latz, J. Phys.: Condens. Matter **1**, 7163 (1989).
[72] E. Overbeck, C. Sinn, and M. Watzlawek, Phys. Rev. E (to be published).
[73] B. Cichocki and B. U. Felderhof, J. Chem. Phys. **94**, 556 (1991).
[74] B. Rinn, K. Zahn, P. Maass, and G. Maret, Europhys. Lett. **46**, 537 (1999).
[75] W. Härtl *et al.*, University of Saarbrücken, Germany (private communication, 1999).
[76] A. P. Philipse and A. Vrij, J. Chem. Phys. **88**, 6459 (1988).
[77] J. K. Phalakornkul *et al.*, Phys. Rev. E **54**, 661 (1996).
[78] W. Härtl, C. Beck, and R. Hempelmann, J. Chem. Phys. **110**, 7070 (1999).
[79] W. B. Russel and A. B. Glendinning, J. Chem. Phys. **74**, 948 (1980).
[80] M. Fuchs, W. Götze, I. Hofacker, and A. Latz, J. Phys. (France) **3**, 5047 (1991).
[81] W. Härtl, H. Versmold, and X. Zhang-Heider, J. Chem. Phys. **102**, 6613 (1995).
[82] D. M. Heyes and P. J. Mitchell, J. Chem. Soc., Faraday Trans. **90**, 1931 (1994).
[83] B. Cichocki and K. Hinsen, Physica A **187**, 133 (1992).
[84] C. W. J. Beenakker, Physica A **128**, 48 (1984).
[85] B. Cichocki and B. U. Felderhof, J. Chem. Phys. **98**, 8186 (1993).
[86] B. Cichocki and B. U. Felderhof, Physica A **204**, 152 (1994).
[87] J. M. Rallison and E. J. Hinch, J. Fluid Mech. **167**, 131 (1986).
[88] J. P. Hansen and L. Verlet, Phys. Rev. **184**, 150 (1969).
[89] H. Löwen, T. Palberg, and R. Simon, Phys. Rev. Lett. **70**, 1557 (1993).